The Composition of Comets

Anita L. Cochran, Anny Chantal Levasseur-Regourd, Martin Cordiner, Edith Hadamcik, Jérémie Lasue, Adeline Gicquel, David G. Schleicher, Steven B. Charnley, Michael J. Mumma, Lucas Paganini, et al.

The Composition of Comets

Anita L. Cochran[1], Anny-Chantal Levasseur-Regourd[2],Martin Cordiner[3],
Edith Hadamcik[4], Jérémie Lasue[5], Adeline Gicquel[3,9],
David G. Schleicher[6], Steven B. Charnley[3], Michael J. Mumma[3],
Lucas Paganini[3], Dominique Bockelée-Morvan[7], Nicolas Biver[7], Yi-Jehng Kuan[8]

1. The University of Texas, McDonald Observatory, Austin, TX USA
2. UPMC, LATMOS, Paris, France
3. NASA Goddard Space Flight Center, Greenbelt, Maryland, USA
4. UPMC, LATMOS, Guyancourt, France
5. UPS, IRAP, Toulouse, France
6. Lowell Observatory, Flagstaff, AZ, USA
7. LESIA, Observatoire de Paris, Meudon, France
8. National Taiwan Normal University, Taiwan, ROC
9. MPS, Göttingen, Germany

Abstract

This paper is the result of the International Cometary Workshop, held in Toulouse, France in April 2014, where the participants came together to assess our knowledge of comets prior to the ESA Rosetta Mission. In this paper, we look at the composition of the gas and dust from the comae of comets. With the gas, we cover the various taxonomic studies that have broken comets into groups and compare what is seen at all wavelengths. We also discuss what has been learned from mass spectrometers during flybys. A few caveats for our interpretation are discussed. With dust, much of our information comes from flybys. They include *in situ* analyses as well as samples returned to Earth for laboratory measurements. Remote sensing IR observations and polarimetry are also discussed. For both gas and dust, we discuss what instruments the Rosetta spacecraft and Philae lander will bring to bear to improve our understanding of comet 67P/Churyumov-Gerasimenko as "ground-truth" for our previous comprehensive studies. Finally, we summarize some of the inital Rosetta Mission findings.

1 Introduction

Comets are leftovers from when our Solar System formed. These icy bodies were formed out of the solar nebula in the outer regions of our Solar System. Many of these bodies were swept up and incorporated into the giant planets. The remnants of planetary formation were either ejected from the nascent Solar System, were gravitationally perturbed to the Oort cloud or remained in reservoirs past the orbit of Neptune. The comets we see today have undergone little change from their primordial states. Comets, therefore, represent important objects to study in order to determine constraints suitable for models of the early solar nebula.

Whipple (1950) first described comets as "dirty snowballs" that are composed of a mixture of ices and dust. The mass is approximately equally divided into ices and dust. As the comets approach the Sun, they are heated and the ices sublime. Since comets are small (generally a few to 10s of km), the resultant gas is not bound to the nucleus and expands outwards into the vacuum of space. When it leaves the nucleus, the gas carries with it some of the solid particles (refractory grains, refractory organics, icy grains, agregates of ice and dust). The resultant material forms the cometary comae (and sometimes tails) that are so prominent when a comet is in the inner Solar System. We do not observe the nucleus composition directly, except when observing from a spacecraft flying past or during a rendezvous mission. What we generally observe is the gas in the coma and the light reflected off the refractories and we *infer* composition from those.

The gases that come directly from the nucleus first flow through a region near the nucleus where the gas densities are sufficiently high that collisions, and thus chemical

reactions, can take place. This so-called "collisional" zone is < 1000 km for all but the most productive comets. With typical outflow velocities near 1 AU of 850 m/sec, this means that the outflowing gas clears this region in the first 20 minutes of outflow. Once out of the collisional zone, photochemical processes change the composition of the gases.

The comets were formed over a wide range of heliocentric distances and conditions. Petit *et al.* (2015, this volume) discuss the dynamics of the formation. In this review, we will discuss what we have learned about the chemical composition of the gas and dust using studies at all wavelengths. Our conclusions will be tempered by some caveats based on some current observations. The subject of isotope ratios, however, will be covered in the review by Bockelée-Morvan *et al.* (2015, this volume). Finally, we will discuss what observations the Rosetta Mission can make to improve our understanding, We include some early results of this mission.

2 Gas Composition

The spectra of comets are mostly composed of emissions from gas-phase molecules superposed onto a continuum that results from sunlight reflecting off dust. Many of the emissions arise from resonance fluorescence of the gas, but prompt emissions also play an important role. Optical spectra of comets have been obtained since the 1860s, while UV, radio and IR spectra have been obtained since the 1970s.

Optical spectra of comets contain few parent species. The spectra are mostly bands of fragment molecules (often called daughters though they can be grand-daughters or chemical products). Thus, the parent species must be inferred using lifetimes and chemical reaction networks. The IR and radio spectra (including mm and sub-mm) contain a mixture of parent and daughter species. Many of the molecules only possess transitions in the IR because they do not have permanent dipole moments. In the UV, we see parents and daughters, as well as a number of important atomic features, such as H, C and O.

Early on, it was noted that the spectra of different comets seemed similar (rarely was an unusual feature noted in the spectra). The strengths of the emission lines relative to the continuum did seem to vary and the relative strengths of bands changed with heliocentric distance. This led to the question of whether all comets shared the same composition or whether there were distinctly different classes of comets. This question is important for our understanding of the homogeneity of the solar nebula at the epoch(s) and the region(s) where comets formed. Thus were born some large comparative studies of comets at all wavelengths in order to understand the chemical homogeneity or diversity of comets. Of course, even if comets formed identically, their spectra might have been altered by activity or irradiation over their lifetime. Thus, we need to look for clues of evolution in the spectra.

2.1 Optical Observations

Since optical observations of comets have existed for far longer than spectra at other wavelengths, there are many more comets observed in the optical than at any other wavelengths. The optical observations consist of high-resolution and low-resolution spectra, as well as photometry obtained with narrow-band filters that isolate the molecular bands. Optical observations are also the most sensitive to faint comets, meaning that the optical observations can be gathered for more comets and at larger heliocentric distances than the other wavelength observations. Additionally, the typical photometric aperture or long slit used is larger than those used in the IR, allowing observations of a larger portion of the coma. The larger the aperture, the less sensitive are the observations to outflow velocity or short term temporal variability (which instead can be measured at other wavelengths). Feldman *et al.* (2004) discuss how to turn optical observations of fragment species into knowledge of the composition of comets.

The spectral observations have the advantage that they can easily isolate the molecular features from the continuum, but suffer from small apertures. Some observers use long-slit spectrographs that allow for measurements of the coma as a function of cometocentric distance. This is an improvement over small apertures and allows direct measurement of scale lengths for decay, but the long slit only allows for sampling in specific directions within the coma. Spectroscopic observations often have significant spectral grasp, so that multiple species can be observed simultaneously, minimizing worries of temporal variability. Large surveys with low-resolution optical spectra have been carried out since the 1970s (Newburn and Spinrad 1984, 1989; Cochran 1987; Fink and Hicks 1996; Fink 2009; Langland-Shula and Smith 2011; Cochran *et al.* 2012) with well over 150 comets observed spectroscopically.

High-resolution studies have tended to focus more on individual cometary properties and are excellent for detailed work. Examples of the types of studies performed are $^{12}C/^{13}C$ (Danks *et al.* 1974; Kleine *et al.* 1995), $^{14}N/^{15}N$ (Arpigny *et al.*. 2003; Manfroid *et al.* 2005, 2009) and O ($^1S/^1D$) (Festou and Feldman, 1981; Cochran and Cochran 2001; Cochran 2008; Capria *et al.* 2005, 2008; McKay *et al.* 2012, 2013, Decock *et al.*, 2013, 2015).

Photometry with filters allows for much larger apertures and is therefore much more sensitive than spectroscopy (Schleicher and Farnham 2004). Continuum removal is done with observations through filters that isolate continuum regions. Large photometric studies of comets have been carried out (A'Hearn and Millis 1980; A'Hearn *et al.* 1995; Schleicher and Bair 2014), with more than 160 comets observed. Photometry suffers from the problem of not being able to measure weak features (e.g. CH or NH_2) because there is a practical limit to how accurately the underlying continuum can be determined and removed.

With photometry, the different filters are observed sequentially, thus temporal variations could change our understanding of the relative abundance of species. However, the cycle time to observe all filters is typically much shorter than the expected timescale for temporal variability. With long-slit spectra, the spectra may be obtained at multiple position angles to sample any inhomogeneities of the coma. At that point, temporal variations must be considered. Typically, the time between position angles is much longer than between filters with photometry.

Without prior knowledge of any asymmetry, single-aperture photometry and small-aperture and long-slit spectroscopy all must assume that the distribution of the gas in the coma is symmetric. This is rarely the case. Examples of asymmetry can be seen in Cochran *et al.* (2012, see Figure 5). While not able to probe the morphology of the coma, these observations are, however, measuring the bulk composition of the nucleus. It is this composition that is the necessary measurement to aid our understanding of the conditions in the solar nebula, while morphology tells us more about the physical condition of the nucleus today. However, morphology also may tell us about inhomogeneities of the nucleus, lending clues to the size and variation in composition of the presumed cometesimals from which the nucleus was assembled.

To some extent, this assumption of symmetry can be mitigated with an integral field unit (IFU) spectrograph, where spectra can be obtained from many positions in the coma at the same time and with spectral resolution sufficient to isolate bands. IFU spectroscopy is not as readily available as other instrument types and most IFU spectrographs have very small fields-of-view. Alternatively, the coma can be imaged with narrow-band filters to measure the morphology of the coma.

Early studies of cometary diversity were carried out by A'Hearn and Millis (1980), Newburn and Spinrad (1984) and Cochran (1987). These papers included measurements of daughters such as CN, C_2, C_3, and O I. All the authors noted that the ratios of species appeared very similar for most comets but there were occasional comets that seemed depleted in C_2 or C_3. However, the sample sizes in these first papers were small and it was not apparent what cometary properties were common to the unusual comets.

Since 1995, several large studies have been published with the total number of comets studied by all groups around 250 (A'Hearn *et al.*. 1995; Fink 2009; Langland-Shula and Smith 2011; Cochran *et al.* 2012; Schleicher and Bair 2014). Many of these comets were observed by more than one group. Additional species were added in these surveys, including OH, NH, NH_2, and CH. From these studies, it has become apparent that the majority of comets really do have very similar relative compositions. However, 25–30% of the comets look different than the rest. As noted in the earlier studies, many of the comets that are different are depleted in C_2 and C_3.

Unfortunately, intercomparing surveys is difficult, since the various authors have used different g-factors and scale lengths in their reductions, as well as different cut-offs

for the definition of depletion. However, the surveys are mostly consistent in comet-by-comet comparisons when they do overlap on the same comet, agreeing which comets show differences. The inconsistent reductions, however, are why ever larger surveys by a single group can make the most progress.

Figure 1 demonstrates that the depletions are not a subtle effect by comparing observations of comets 21P/Giacobini-Zinner (GZ) and 8P/Tuttle when both were near 1 AU from the Sun and 0.5 AU from Earth. The Tuttle spectrum demonstrates the full, normal, range of observed molecules. GZ is the prototypical depleted comet and it is clear that there is much less C_3/CN and C_2/CN in GZ than in Tuttle.

After the earliest studies, it seemed that the depletion occurred primarily in Jupiter Family comets. However, the studies of A'Hearn *et al.* (1995), Fink (2009), Langland-Shula and Smith (2011) and Cochran *et al.* (2012) had sufficiently large samples that it became apparent that the relationship between dynamical state and depletion was not so simple. These studies showed that depleted comets can be from any dynamical type: Jupiter Family, Halley Type, Long-period (dynamically new and not). However, it is more common for depleted comets to be Jupiter Family comets; Cochran *et al.* (2012) found that two thirds of the depleted comets were Jupiter Family while one third were long period. In addition, a higher percentage of the Jupiter Family comets (37%) were depleted than of the long period comets (18.5%). Thus, the depletion is either pointing to different evolutionary states or it is pointing to mixing of the formational reservoirs.

Cochran *et al.* (2012) pointed out that the picture is a little more subtle than just "carbon-chain depleted" or "typical". The definitions for carbon-chain depletion typically only account for C_2 relative to OH or CN and it is these C_2-depleted comets that represent 25–30% of all comets. However, Cochran *et al.*. found that only $\sim$ 10% of comets are depleted in both C_2 and C_3. They also found some number of comets with different patterns for some other molecules, but the statistics did not warrant breaking the comets into additional groups.

Schleicher and Bair (2014) have analyzed photometry of 167 comets observed and reduced in a consistent manner. Of that sample, 101 were of sufficient quality that they were able to be included in the analysis of the statistics of the sample. They find the typical carbon-chain depletions found by other authors. However, their statistics are better than previous studies and they now claim that there are 7 classes of comets: 1) typical (still $\sim$ 70% of comets); 2) comets depleted in both C_2 and C_3 with the depletion as strong as GZ or stronger; 3) comets depleted in both C_2 and C_3 but weaker than the GZ depletion; 4) comets depleted in C_2 but not C_3 (in agreement with Cochran *et al.* 2012); 5) comets depleted in C_3 but not C_2; 6) comets depleted in NH but not depleted in any carbon species; and 7) comets depleted in CN relative to C_2 and C_3 but still depleted in C_2 and C_3 compared to OH (a class of 1 – 96P/Machholz 1; Schleicher 2008).

With the most recent findings, especially that certain depletions are not confined to a single dynamical type, the question of formation vs. evolution is important. One of the best constraints on this question is comet 73P/Schwassmann-Wachmann 3 (SW3). In 1995, comet SW3 underwent a splitting event into three pieces; subsequently, those pieces split again. SW3 is a strongly C_2 and C_3 depleted comet and thus has a distinctive "fingerprint". If the depletion were just an evolutionary effect, from multiple perihelion passages, we would expect it to be confined mostly to the surface and the interior would appear typical. However, observations of the distinct pieces during the 2006 apparition showed that all the pieces had identical depletions both in the parents observed in the IR and the daughters observed in the optical and IR (Kobayashi *et al.* 2007; Jehin *et al.* 2008; Schleicher and Bair 2011). In addition, there was no change from measurements of SW3 obtained before the splitting in 1995 (Schleicher and Bair 2011). This has been interpreted as strong evidence that C_2 and C_3 depletions are primarily from the formation of the comets, not from their subsequent evolution.

2.2 UV Observations

The UV part of the spectrum of comets is not as well studied as the optical because the Earth's atmosphere precludes observations from ground-based telescopes (the OH (0,0) band at 3080Å is technically in the UV but can be observed from the ground; however the atmospheric extinction at this wavelength is typically around ~ 1.5 mags/airmass). Thus, UV observations require a spacecraft-borne telescope or a rocket experiment. The electronic bands of some diatomic molecules are visible in the FUV; atomic daughter products that result from solar UV dissociation are also seen.

In the UV, transitions of CO, H, H_2, O, C, OH, CS and S_2 have been regularly detected. Most of these species are products of a parent molecule, though the processes to produce them are dependent on the transition. Whether S_2 is a parent or a daughter is still unknown.; regardless S_2 is very short-lived. CO is seen to have two different band series, the fourth positive bands and the Cameron bands. The fourth positive bands are the result of solar pumped fluorescence of CO. The Cameron bands result from either electron impact on CO or dissociative excitation of CO_2, the latter being more important. Thus, these two bands can yield information on two possible parents.

The UV era of cometary observations started in 1970 with the Orbiting Astronomical Observatory (OAO-2) observations of comet Bennett (Code *et al.* 1972). In these observations OH and Ly α, both daughters of H_2O, were detected.

Significant progress in our understanding of the UV spectra of comets came with the International Ultraviolet Explorer (IUE) satellite. Ultimately, IUE was used to observe more than 50 comets between 1978 and 1996. Festou (1998) summarized the findings from these observations. He concluded that "with the exception of the S_2 molecule,

new and long-period comets have a chemical composition that does not differ by more than a factor of two from that of periodic comets" (but see discussion below).

Since 1990, the UV has been covered with the Hubble Space Telescope (HST) and a variety of instruments. Also operational during this period, the Far Ultraviolet Spectroscopic Explorer (FUSE) mission operated from 1999 – 2007 and the Galaxy Evolution Explorer (GALEX) operated from 2003. Of these three missions, HST has been the workhorse, having been used to observe many comets.

FUSE was used to observe the FUV from 900 – 1200Å in four comets. In that bandpass, emissions due to H I, O I, CO (including three new Hopfield-Birge band systems), H_2 and N I were detected. A He I resonance transition at 584Å was seen in second order and was taken as an indicator of solar wind charge transfer in the coma. Ar and N_2 were searched for but not detected (Feldman 2005; Feldman *et al.* 2009). In addition, FUSE detected many lines that were initially unidentified, but were later determined to be H_2 (Liu *et al.* 2007).

The GALEX satellite uses time-tagged images and grism mode to obtain both FUV and NUV observations. The FUV observations have concentrated on C I. The NUV is used to observe OH, CS and CO^+ (Morgenthaler *et al.* 2009). Comets fill the field-of-view of the GALEX detector so it is difficult to estimate the background. Morgenthaler *et al.* (2011) describe the process of extracting the C I lifetime from observations of comet C/2004 Q2 (Machholz). They found that either the CO lifetime is shorter than previously thought or another shorter-lived species must be contributing to the production of C I in the inner coma.

Using the FIMS/SPEAR instrument on the Korean STSAT-1, Lim *et al.* (2014) observed comet C/2001 Q4 (NEAT) in the FUV. They observed the CO fourth positive bands as well as C I and S I atomic features. They concluded that the production rate of C is $\sim 60\%$ of CO, agreeing with results obtained for other comets, e.g. Morgenthaler *et al.* (2011) for comet C/2004 Q2 (Machholz). For comet NEAT, Lim *et al.* found that S I production was about 1% of the water production rate. It was assumed the parent was H_2S.

Meier and A'Hearn (1997) had already published a study of S I in 19 comets observed with IUE and HST. They also observed CS in these spectra, presumably a daughter of CS_2. Typical values for CS_2 derived are not sufficient to supply all of the S. Meier and A'Hearn pointed out that all the transitions they see are optically thick. This means that simple fluorescence models are not sufficient and they developed a radiative transfer/collisional model to interpret their spectra. For the comets they studied, Meier and A'Hearn derived sulfur abundances of 0.1% to 1% relative to water.

HST has observed 18 comets with a variety of instruments. The comets are a mixture of Jupiter Family and long-period comets. Comet 103P/Hartley 2 (the target

of the EPOXI mission) was observed with HST during three different apparitions (1991, 1998, 2010), the only comet observed over more than one apparition. With most of these observations, the CO fourth positive bands and the OH bands are observed simultaneously, thus enabling a measure of the CO:H_2O for many comets. Lupu *et al.* (2007) presented models of the CO fourth positive bands in four comets observed with HST. These observations showed a large range of Q_{CO}/Q_{H_2O}, from $< 1\%$ for C/2000 WM1 (LINEAR) to $> 20\%$ for comet C/1996 B2 (Hyakutake).

Since then, Weaver *et al.* (2011) have reported that comet 103P/Hartley 2 had a CO/H_2O production rate ratio of $0.15 - 0.45\%$, amongst the most carbon monoxide poor comets measured. The temporal variation in CO abundance was seen to correlate with the rotation of the comet. It should be remembered that A'Hearn *et al.* (2011) detected strong CO_2 ($CO_2/H_2O \sim 20\%$) with the EPOXI spacecraft at a similar time. Thus, Hartley 2 is CO_2 rich while CO poor.

Weaver *et al.* noted that CO/H_2O varies by a factor of 50 across all comets observed to date using UV data. This is in agreement with IR observations (e.g. Paganini *et al.* 2014b). Though the most CO-rich comets are long period comets, not all long period comets are high in CO (e.g. C/2000 WM1 (LINEAR) is very low). Even though CO can be produced as a daughter product of species such as CO_2 or H_2CO, Weaver *et al.* concluded that the HST high spatial resolution suggests that the CO observed by HST originates from the nucleus.

The Solar Wind ANistropies (SWAN) all-sky Ly α camera on the Solar and Heliospheric Observatory (SOHO) mission has been used regularly to monitor comets since its launch in 1995. Hydrogen is a dissociation product of many species, the most notable of these H_2O. To date, SWAN has been used to observe over 60 comets. These comets are either observed as routine interlopers in the all-sky images or can be specifically targeted for monitoring. With its orbit at the L1 Lagrangian point, SOHO with SWAN is able to observe comets at very small heliocentric distances as well as north and south of the ecliptic. When a comet is very near to the Sun, the lifetime of H_2O against photodissociation is extremely short and water dissociates completely within the collisional zone. Examples of comets observed close to the Sun are C/2002 V1 (NEAT), C/2002 X5 (KudoFujikawa), 2006 P1 (McNaught) and 96P/Machholz 1 (Combi *et al.* 2011). The closest passage to the Sun by a comet observed by SOHO came in fall 2013 when comet C/2012 S1 (ISON) broke up within a few solar radii, hours before perihelion (Combi *et al.* 2014).

While the SWAN observations tell us only about the water production rate of comets and not of other species, they are extremely valuable for being able to monitor the production rates of comets as they approach and recede from the Sun. Combi *et al.* (2011) pointed out that there are two types of behaviors: comets whose water production rate increases with a steep slope as they approach the Sun and those with a more shallow

slope. However, they pointed out that all of the steep-sloped comets are Jupiter Family comets of the type that have typical perihelia near 1 AU. Indeed, the only periodic comets in the moderate-slope group are 153P/Ikeya-Zhang and 96P/Machholz 1. Neither is a Jupiter Family comet. Ikeya-Zhang has a ~ 350 year period. Machholz 1 is in a highly inclined (58°) orbit.

2.3 IR Observations

The lack of a permanent dipole moment in many of the cometary parent molecules means that these molecules cannot be observed in the optical or radio; they have strong vibrational transitions in the IR. Studies of these spectral regions were not possible until the 1970s when IR detectors were introduced to astronomy. The first detectors were not very sensitive and were also very small.

The IR offers some difficult challenges not seen in the optical part of the spectrum. The Earth's atmosphere has significant opacity in the IR due to molecules such as CO_2 and H_2O. Thus, there are broad regions of the atmosphere that are opaque to the cometary photons. This means that we can only study molecules that occur in "clean" regions of the spectrum. It also argues for higher spectral resolution to avoid bad regions of the spectrum. Even the clean regions have significant, and variable, opacity so the atmosphere must be carefully measured, with equal amounts of observation time on sky and comet, and the atmosphere must be modeled and removed. Figure 2 demonstrates the importance of high spectral resolution for IR work.

Most of the IR observations are in the 1–5μm region, with most of the interest in the 2.5–5μm bandpass. IR observations are typically limited by the regions in the Earth's atmosphere that are most transparent. Doppler shifts of cometary lines can move them from the good region into the more opaque regions of the bandpass. Limitations on time available to observe and the spectral grasp can lead to different molecules being detected for different comets.

A variety of species in the IR spectra of comets have been detected, including H_2O, CH_4, C_2H_2, C_2H_6, H_2CO, NH_3, CH_3OH, HCN, etc. All of these are seen in molecular clouds. However, there are still some species seen in molecular clouds and not comets. In addition to the parent species seen in the IR, fragments such as OH, NH_2 and CN are observed. Dello Russo *et al.* (2013) include a high-resolution atlas of comet 103P/Hartley 2. The first such infrared spectra of a comet obtained with a cross-dispersed echelle spectrometer appeared in Mumma *et al.* (2001) for comet C/1999 H1 (Lee). A complete spectral atlas for comet Lee appeared in Dello Russo *et al.* (2006).

Determining production rates from IR spectra requires taking into account the various excitation processes. These are discussed in detail in Bockelée-Morvan *et al.* (2004).

As with the optical models, differences in model parameters can make intercomparing results a bit problematic. In recent years, intense activity has led to greatly improved fluorescence models for primary volatiles in comets and improved transmittance models for the terrestrial atmosphere (e.g. DiSanti *et al.*, 2013; Gibb *et al.*, 2013; Kawakita and Mumma, 2011; Lippi *et al.*, 2013; Radeva *et al.*, 2011; Villanueva *et al.*, 2012).

The sample of comets observed in the IR is much smaller than the sample in the optical because the IR observations require bigger telescopes and the IR cannot be used to observe the fainter comets. In addition, IR observations are generally obtained over a smaller range of heliocentric distances than, for example optical data, because the comets are fainter far from the Sun. This is rapidly changing. Paganini *et al.* (2013) detected CO in the unusual comet, 29P/Schwassmann-Wachmann 1 at 6.26 AU. At this point, about three dozen comets have been observed in some part of the IR.

IR observations are scattered over many papers that concentrate on a single or a few comets, with brief mention of groupings of comets. Since 2013, papers have been published on 2P/Encke (Radeva *et al.*, 2013), 21P/Giacobini-Zinner (DiSanti *et al.*, 2013), 81P/Wild 2 (Dello-Russo *et al.*, 2014b), 103P/Hartley 2 (Kawakita *et al.*, 2013; Dello Russo *et al.*, 2013, Bonev *et al.*, 2013), C/2003 K4 (LINEAR) (Paganini *et al.*, 2015) C/2009 P1 (Garradd) (DiSanti *et al.*, 2014), C/2010‘G2 (Hill) (Kawakita *et al.*, 2014), C/2012 F6 (Lemmon) (Paganini *et al.*, (2014a), C/2012 S1 (ISON) (Bonev *et al.*, 2014), and C/2013 R1 (Lovejoy) (Paganini *et al.*, 2014b). Inspection of this list shows that it is a mix of long-period and Jupiter Family comets. However, it has been much harder to observe Jupiter Family comets in the IR since they generally are at the faint end of detectability.

From the IR observations, there is an emerging picture that there are three different kinds of comets: typical, organic enriched and organic severely depleted (c.f. Mumma and Charnley 2011). However, as Mumma and Charnley pointed out, taxonomies based on optical fragments and IR primary species are not always in agreement. As an example, 8P/Tuttle, a Halley Type Comet, is found to be typical in C_2/CN in the optical but peculiar in the IR because C_2H_2 and HCN are severely depleted and C_2H_6 is low, in contrast to CH_3OH that is enriched (Bonev *et al.*,2008).

The limited windows through the atmosphere that ground-based IR observations must use mean that important parents cannot be observed from the ground. The most important is CO_2. CO_2 is important because it represents a significant fraction of the ice (around 20% is not uncommon). CO_2 is also much more volatile than H_2O. Thus, while the activity of comets is controlled by the sublimation of water inside $\sim$ 3 AU, outside of this region, it is CO_2 or CO that control the activity (CO can either be a daughter or a parent). Observations obtained with the AKARI spacecraft demonstrate this point, showing that the CO_2 abundance relative to H_2O is much higher outside of 2.5 AU (Ootsubo *et al.* 2012). Some comets were observed both outside and within

$\sim$ 2.5 AU and the driver of activity is shown to change. No evidence was seen for a difference between Jupiter Family and long-period comets.

Reach *et al.*. (2013) used the Spitzer Space Telescope to determine the amount of CO_2 relative to H_2O. While many of the Spitzer-observed comets look to have abundances similar to the AKARI comets, Reach *et al.* found a number of comets that were CO_2 poor. Those CO_2 poor comets are a mix of optically classified typical and depleted comets. Reach *et al.* concluded that more of the CO_2 poor comets were depleted than typical comets but they did not have taxonomic classifications on several of the CO_2 poor comets. With recent photometric observations, it turns out that the CO_2 poor comet group contains 3 depleted comets, 5 typical comets and 1 unclassifiable comet (Schleicher 2015, personal communication). It should be noted that while the AKARI observations are spectral, the Spitzer observations were imaging observations. The filter that contains the CO_2 also contains a considerable quantity of dust that was measured with a nearby continuum filter. Depending on the dust properties, it is possible that some of the noted depletions are instead dust contamination.

While the AKARI and Spitzer spacecraft have been used to look at a large number of comets, these spacecraft are available for observations for only a limited amount of time. McKay *et al.* (2012, 2013) and Decock *et al.* (2013, 2014) have used discussions of branching ratios for the processes to produce [O I] (e.g. Festou and Feldman, 1981) and have developed procedures and empirical release rates to use observations of the forbidden oxygen lines in the optical to *infer* the abundance of CO or CO_2. This is done by looking at the ratio of the O(^{1}S) (or green) line to the sum of the O(^{1}D) (or red) pair of lines. Unfortunately, this method relies on lifetimes and branching ratios that are not well determined in the lab and calibration against the IR is sorely needed.

A key use of IR spectra has been to map the ortho/para ratio of the gas for a variety of molecules. If a molecule has H atoms that are located symmetrically, then these molecules may have states that have different spin orientations of the hydrogen. As an example, for H_2O, the two H atoms can have their spin orientation the same or opposite one another. The first of these orientations is known as the "ortho" state, while the second is the "para" state. A unique feature of the spin states is that it is not possible to flip the state by radiative or collisional processes. Thus, the ortho/para ratio (OPR) of the coma gas measures the ortho/para ratio of the gas reservoir when the gas was frozen into the nuclear ices. Measurement of the rotational distribution in each spin species can lead to a measurement of the ortho/para ratio and thus to the nuclear spin temperature. Since most of these molecules reach equilibrium at some temperature, the ortho/para ratio measures the spin temperature of the ice (but see below). Bockelée-Morvan *et al.* (2004) discuss how these conversions are achieved.

Mumma *et al.* (1987) were the first to measure an OPR in H_2O for a comet. Since then, about a dozen OPRs in water have been measured. Mumma and Charnley (2011)

summarized the values through 2011. Recently, Bonev *et al.* (2013) and Kawakita *et al.* (2013) used this technique to study the spin temperature in H_2O for comet 103P/Hartley 2. As discussed in these papers, they found a range of ratios that did not always agree within the error bars. However, in general, it appeared that T_{spin} was below 40 K.

Shinnaka *et al.* (2011) presented OPRs in NH_2 (optical) and NH_3 (IR) for 15 comets. They found the same value for most comets, with SW3 standing out as being different. Occasionally, OPRs can be measured in other species (e.g. CH_4, c.f. Mumma and Charnley 2011). These observations, however, are rarer because they rely on being able to observe the comets at critical Doppler shifts. In eight comets, spin temperatures for NH_3 and H_2O were relaxed and in agreement; spin temperatures for methane also agreed when co-measured with H_2O or NH_3 (c.g. Mumma and Charnley, 2011).

The use of OPRs was believed to be a sensitive measure of the formational temperature of the ice. However, recent laboratory experiments (Fillion *et al.* 2012) pointed out that the speed of desorption has a major affect on this ratio. Thus, it remains to be seen how useful OPRs are as constraints on temperature in the solar nebula vs. as taxonomic tools.

2.4 Radio Observations

Pure rotational transitions for molecules with dipole moments occur in the radio portion of the spectrum. These simpler transitions make it easier to detect complex volatiles. In addition, radio spectroscopy has very high spectral resolution, allowing for accurate measurements of spectral line shapes and Doppler shifts in the cometary coma. Thus, with radio observations it is possible to measure the line-of-sight outflow velocity of the coma. Radio telescope beams tend to be very large. Thus, the radio observations measure the total abundance of a species but have to assume the outflow is symmetric. Mapping may be obtained by shifting the beam center, though the additional positions are generally limited in number. The mapping can be improved upon with interferometry (see subsection 2.4.1).

The earliest radio observations were made of the daughter species, OH, at 18cm. Since 1973, there have been more than 50 comets observed with the Nançay telescope (Crovisier *et al.* 2002; Colom *et al.* 2011).

There are more than a dozen species seen in the radio in comets. Species such as CO, H_2CO, CH_3OH, CH_3CN, HC_3N, HCN, NH_3, HCOOH, HNCO, and H_2S are thought to be primary (parent) volatiles. OH, CS, and HNC are likely to be product species. As with the IR, all of these species cannot be observed simultaneously so we have detections of these species in some comets but not others. Thus, though more than 40 comets have

been observed in the radio, very few species have been observed in more than 10 comets (Figure 1 of Crovisier *et al.* 2009 gives an indication of the number of molecules seen per comet for different types of comets).

The comet with the record for the most species observed is C/1995 O1 (Hale-Bopp). This comet's brightness allowed for the detection of molecules that had never before (or since) been seen and measurement of the behavior of the species with heliocentric distance (Biver *et al.* 1997, 2002; Bockelée-Morvan *et al.* 2000). In addition to the molecules mentioned above, SO_2, H_2CS, NH_2CHO, CH_3CHO, and $HCOOCH_3$ were detected. The most complex molecule detected in the spectrum of Hale-Bopp was HO-CH_2CH_2-OH (ethylene glycol) (Crovisier *et al.*. 2004).

Hale-Bopp was an exceptionally bright comet, with a very high water production rate. Indeed, it was the brightest comet since the radio and IR techniques have become mature and routine. Therefore, it was possible not only to observe more molecules in Hale-Bopp than in other comets, but also to observe them over a larger range of heliocentric distances. Most species were observed out to distances of 3–4 AU. However, HCN and CH_3OH were both observed to 6 AU and CO was observed at 14 AU, some four years after perihelion (Biver *et al.* 2002). Figure 5 of Biver *et al.* shows the trends of the production rates of nine molecular species as a function of heliocentric distance, both pre- and post-perihelion. It is obvious from this figure that at large heliocentric distances the CO is controlling the cometary activity, while within about 3 AU the H_2O sublimation is driving the activity.

Crovisier *et al.* (2009) explored the radio-derived abundances of several species relative to water for about 30 comets. They found no evidence for the three categories of typical, depleted and enhanced comets seen in the IR, nor did they detect a difference between Jupiter Family and other dynamical types of comets. They noted that there is a wide spread of abundances relative to water for most species. The exception to this is for their observations of HCN, which, according to Crovisier *et al.*, show a narrow range of values. Figure 3 shows the range of abundance values, relative to water, found in the IR and radio for a number of comets.

2.4.1 The Rise of Radio Interferometry

Combining the benefits of high spectral resolution with simultaneous spatial mapping, radio interferometry is a powerful technique for probing the distribution and kinematics of cometary gas and dust (eg. Blake et al. 1999; Boissier et al. 2014). Currently in Cycle 2 Early Science mode, the Atacama Large Millimeter/submillimeter Array (ALMA) is a state-of-the-art radio/sub-mm interferometer under construction at 5 km altitude in Chile's Atacama Desert. Once completed in 2015-2016, using 66 antennae separated on baselines up to 16 km, extremely detailed mapping of molecular line and continuum

emission from cometary comae will be possible across the frequency range 84-950 GHz, with an angular resolution up to $\sim 0.005''$. Cordiner *et al.* (2014) first demonstrated the power of ALMA for quantitative measurements of the distributions of molecules and dust in the inner comae of typical bright comets, with spectrally and spatially-resolved maps of HCN, HNC, H_2CO and 0.9 mm dust continuum in C/2012 F6 (Lemmon) and C/2012 S1 (ISON).

Observations of these two Oort-Cloud comets were made using the ALMA Band 7 receivers, covering frequencies between 338.6 and 364.6 GHz (0.82-0.89 mm) using 28-30 12-m antennae (with baselines 15-2700 m, which provided an angular resolution of approximately $0.5''$). Comet Lemmon was observed post-perihelion on 2013 June 1-2 at heliocentric distance $r_H = 1.75$ AU and ISON was observed pre-perihelion on 2013 November 15-17 at $r_H = 0.54$ AU. The spectral resolution was about 0.42 $\mathrm{km\,s^{-1}}$. For further details see Cordiner *et al.* (2014).

Figure 4 shows spectrally-integrated flux contour maps for the observed molecules in each comet. Dramatic differences are evident between different molecular species observed in the same comet, and between the same species observed in the two comets. By eye, the HCN distributions in both comets appear quite rotationally-symmetric about the central peak. For Lemmon, no offset between the HCN and continuum peaks is distinguishable, whereas ISON's HCN peak (indicated with a white '+') is offset 80 km eastward from the continuum peak (white '×'). Shown in Fig. 4b, the HNC map for ISON exhibits a wealth of remarkably extended spatial structure, with at least three streams (identified at $> 6\sigma$ confidence), emanating away from the main peak (indicated with white dashed arrows). The majority of HNC emission from both comets is asymmetric, originating predominantly in the anti-sunward hemispheres of their comae.

Formaldehyde also shows strikingly different distributions for comets Lemmon and ISON (Figs. 4c and 4f), highlighting the complex origin of this species. Lemmon has a remarkably flat and extended H_2CO map, as demonstrated by the size of the region traced by the 40% contour compared with the other maps. By contrast, the H_2CO distribution for comet ISON is dominated by a strong, much more compact central peak, and has a relatively symmetrical contour pattern, similar to that of HCN.

Using the method of Boissier *et al.* (2007, 2014), Cordiner *et al.* (2014) modeled the interferometric visibility amplitudes for the observed species in order to determine their origins within the coma. In both comets, HCN was found to originate from (or within a hundred km of) the nucleus, with a spatial distribution largely consistent with spherically-symmetric, uniform outflow. By contrast, the HNC and H_2CO distributions were consistent with the release of these species as coma products. The H_2CO parent scale length was found to be a few thousand km in Lemmon (at $r_H = 1.75$ AU) and only a few hundred km in ISON (at $r_H = 0.54$ AU), consistent with destruction of the H_2CO precursor by photolysis or thermal degradation at a rate which scales in proportion to

the solar radiation flux. The scale length for the putative parent of HNC in comet ISON was found to be $\sim$ 1000 km.

The release of HNC and H_2CO as product species implies the existence of organic precursor materials in the coma, which undergo sublimation, photochemical and/or thermal degradation to produce the observed molecules in the gas phase. Heating or photolysis of materials such as grains, polymers or other macro-molecules, and their subsequent breakdown at distances $\sim$ 100-10,000 km from the nucleus presents the most compelling hypothesis for the origin of the observed H_2CO and HNC. The presence (and composition) of the hypothesized macro-molecular precursors will be measured by the COSIMA instrument on the Rosetta spacecraft during its encounter with comet 67P/Churyumov-Gerasimenko in 2014-2015 (Kissel *et al.* 2007; Le Roy *et al.* 2012).

As ALMA's construction and commissioning are completed over the next two years, the array will grow larger and even more sensitive, enabling the distributions and kinematics of individual coma gases to be resolved on smaller scales than have ever been achieved before; detections of new species should also be possible. Such observations are expected to yield further fundamental new insights into our understanding of cometary compositions.

2.5 Caveat: What About Comets Near the Sun?

The taxonomic studies discussed above generally refer to comets that are at 1 AU or larger heliocentric distances. While we have evidence for a change of the volatile species that controls activity at distances greater than $\sim$3 AU (generally CO or CO_2) compared with within $\sim$3 AU (H_2O), we rarely get to study comets within the orbit of the Earth. Those that we do get to study are generally outside the orbit of Venus. And it is rarer still to observe a comet outside 1 AU and follow it inside the orbit of Mercury.

In fall 2013, we got just such an opportunity with comet C/2012 S1 (ISON). ISON was the very rare Sun-grazing comet that was discovered well in advance of its perihelion passage (and subsequent destruction in this case). At larger heliocentric distances, optical observations showed this comet to be typical in some species, depleted in others and even enhanced in some species. IR observations of C_2H_2 and HCN seemed typical; CH_3OH, C_2H_6 and CH_4 were depleted; NH_3 was enhanced (Dello Russo *et al.*. 2014a; DiSanti *et al.* (2015). Stranger still, DiSanti *et al.* noted that the H_2CO started out depleted, trended to typical and ended up enriched as the comet went from $>$ 1 AU to $<<$ 1 AU. Figure 5 shows what happened in optical spectra as a function of time (McKay *et al.* 2014). With the exception of NH_2, the normal fragment molecules appear to have increased in production relative to water as the comet moved well inside of 1 AU. Opitom *et al.* (2014) saw similar behavior for C_2 and CN production relative to OH using the TRAPPIST telescope monitoring the comet from 1.3 $\rightarrow$ 0.3 AU inbound. In addition,

examination of the top row of the ALMA data in Figure 4 shows that there are large differences in the distribution of the different species.

2.6 Mass Spectrometer Measurements

All of the above discussion was based on remote-sensing observations of comets and includes observations of several hundred comets. Ideally, one would like to take samples of the ices back to the laboratory for measurement, especially if they could be kept in the ice state so that the structure could be preserved and chemistry prevented. However, sampling and transporting a sample back to the lab is a process that is still on the horizon. Alternatively, one can take the laboratory to the comet. The Rosetta mission is doing just that, with samples of the coma from the main spacecraft and samples of the ice from the Philae lander.

Prior to Rosetta, *in situ* direct measurements of the cometary material with a mass spectrometer have only been accomplished once, for comet 1P/Halley. The Giotto spacecraft was successful in sampling the coma during its flyby and analyzing the composition. The results of this have been discussed by Eberhardt (1999). It was the Giotto mass spectrometer that first measured many primary volatiles leading to a detailed comparison of relative abundances. Figure 6 graphically shows the values, taken from Table 1 of Eberhardt, for the abundances of the ten molecules detected as direct contributions from the nucleus for comet Halley. There are also two upper limits. In addition, this experiment showed that some species, CO and H_2CO, that were directly produced at the nucleus, also resulted from an extended source (however, note that the spacecraft was never closer to the nucleus than 110 km so had no spatial information closer than that). CO obviously could be a parent as well as a daughter of CO_2, but the H_2CO extended source is rarely seen in comets (but see Subsection 2.4.1 above). However, as Eberhardt pointed out, the lack of detection of two sources from the ground-based observations is more a function of the difficulty of differentiating the sources at the spatial scale of the ground-based observations. The first measurements of the D/H ratio in H_2O were obtained (with IMS and NMS on-board Giotto), providing D/H values of about 3×10^{-4} (Balsiger *et al.*, 1995; Eberhardt *et al.*, 1995).

While these mass spectrometer observations of Halley are direct measurements, it should be remembered that they were still measuring the coma gas after it had flowed off the nucleus. Thus, some of the species had already undergone some chemistry and photo processes. In addition, the nature of a mass spectrometer means that there will be break-up of some of the species going through the instrument. Thus, to interpret the measurements of the complex mass spectrum, one needs a detailed model of the *expected* abundances to match. This is especially true of species that are available at the percent level or lower. In addition, depending on the mass resolution of the instrument, there

is a limit on differentiating species of similar mass. An important example is CO vs. N_2, both at 28 amu. The Rosina spectrograph onboard Rosetta has improved resolution from the Giotto instruments but still relies on a model to interpret some of its results.

2.7 Gas Composition: Rosetta Capabilities and Early Results

There are instruments on both the Rosetta orbiter and Philae lander designed to determine the composition of the coma. These range from remote sensing cameras with filters or spectrometers to coma-sniffing mass spectrometers.

On the orbiter, ROSINA (Rosetta Orbiter Spectrograph for Ion and Neutral Analysis; Balsinger *et al.* 2007) is a mass spectrometer with three parts: DFMS (Double Focusing Mass Spectrometer, a high mass resolution spectrometer); RTOF (Reflectron Time-of-Flight Mass Spectrometer, a high mass range spectrometer) and COPS (pressure sensor to measure the total and ram pressure). DFMS can be used in restricted ranges to separate critical species such as ^{13}C vs. CH or CO vs. N_2. RTOF can identify organic molecules, such as PAHs. MIRO (Microwave Instrument for the Rosetta Orbiter; Gulkis *et al.* 2007) is used to monitor H_2O, CO and CO_2 abundances. Alice (Stern *et al.* 2007), a UV imaging spectrometer, monitors coma features such as the CO fourth-positive system, Ly α, O, as well as scans the surface. VIRTIS (Visible and Infrared Thermal Imaging Spectrometer, Coradini *et al.* 2007) is used to determine the composition of the ices on the surface of the nucleus. These instruments will be used over a wide range of heliocentric distances as the spacecraft flies alongside the comet from rendezvous through perihelion.

On the lander, samples are analyzed with COSAC (COmetary SAmpling and Composition Experiment; Goesmann *et al.* 2007) and Ptolemy (Wright *et al.* 2007). COSAC is an evolved gas analyzer that will concentrate on elemental and molecular composition. Ptolemy is an evolved gas analyzer that will ephasize measuring the isotopes. The length of time that the lander can be used to sample the gas depends upon power replenishment for the batteries. On the original descent to the surface, the lander bounced several times and was only able to send back a limited amount of data. However, the lander has communicated with the ground again after the comet got closer to the Sun, starting in June 2015.

Early results from these instruments have shown a wealth of detail. MIRO detected the ground-state rotation line of H_2O in June 2014, when the comet was 3.9 AU from the Sun (Gulkis *et al.*, 2015). This was a blue-shifted asymmetric line, indicating that it came from the day side of the comet. MIRO observations showed that the surface was very insulating.

Early ROSINA observations showed that the density of gas varied with the rotation

period and the latitude. CO_2 and H_2O varied with different rotational phases; the CO_2 and H_2O arise from different places on the nucleus (Hässig *et al.*, 2015). The ratio between H_2O, CO and CO_2 varies quite substantially along the spacecraft trajectory. ROSINA was also used to detect various isotopes of H and O (Altwegg *et al.*, 2015) The D/H was higher than other comets. ROSINA was able to detect both CO and N_2, with modeling needed to derive abundances (Rubin *et al.*, 2015). They found that N_2/CO is severely depleted relative to the protosolar values.

Together, the orbiter and lander observations provide "ground-truth" about comet 67P/Churyumov-Gerasimenko (CG). We already know from ground-based observations that CG is one of the carbon-chain depleted comets. It will take all of the observations of comets detailed in previous sections to place CG into context.

3 Solid Particle Composition and Properties

This section summarizes our understanding of the composition of solid particles in cometary comae. It is derived from flybys performed prior to the Rosetta rendezvous, from Earth (or Earth's orbit) remote spectroscopic and polarimetric observations of various comets, e.g., comet 1P/Halley, the first to experience a close spacecraft flyby, comet C/1995 O1 (Hale-Bopp), a very active Oort cloud comet, and some rather bright Jupiter family comets (JFCs). Solid particles are ejected with gases whenever the surface of a nucleus is close enough to the Sun to allow ice sublimation. Solid components in cometary comae appear to be mostly composed of refractory materials such as silicates, organics and amorphous carbon. Refractory dust particles present mixtures of different mineralogies. Icy grains, which rapidly evaporate, and semi-refractory carbonaceous components that suffer photolysis, may also be found in inner cometary comae.

3.1 Evidence from Cometary Flybys

3.1.1 1P/Halley flybys: First Discoveries on Cometary Dust Composition

Major discoveries came from the dust mass spectrometers on board Vega 1 and 2 (PUMA) and Giotto (PIA) spacecraft in March 1986. The relative velocity of the probes and comet Halley on its retrograde orbit was so high (about 70 km s^{-1}) that only information on the atomic composition could be obtained (Kissel *et al.*, 1986a,b). From spectrometric analyses (mostly PUMA 1), dust particles were found to consist not only of a mixture of major rock-forming elements (e.g., silicates, metals, sulphides, with Mg, Si, Ca, Fe), but also, quite unexpectedly, of carbon-hydrogen-oxygen-nitrogen compounds, the so-called "CHONs". The presence of large polymers of organic molecules was also suspected from

the positive ion cluster composition analyzer (with RPA on-board Giotto), the most refractory polymers being likely part of dust particles (e.g., Krueger *et al.*, 1991), and from the three-channel spectrometer (TKS) on board Vega 2 (e.g., Moreels *et al.*, 1994). It was suggested that some gases detected in the coma were degradation products of polymers of formaldehyde on cometary solid particles (Cottin *et al.*, 2004).

The very low geometric albedo of the nucleus surface, of about 4% (e.g., Keller *et al.*, 1986), was also a clue to a highly porous surface, with its slightly reddish color suggesting the presence of dark organic compounds. Moreover, local data on dust impacts (from the DID instrument) and on light scattered by dust (from the OPE instrument) could be compared along the Giotto trajectory (Levasseur-Regourd *et al.*, 1999). These two *in situ* data sets, with their similarities and correlations, offered a diagnostic test of the validity of cometary coma models. Significant increases in local intensity and decreases in polarization for distances to the nucleus below 2000 km suggested the presence of small icy particles in the innermost coma. (Levasseur-Regourd *et al.*, 1999). Fits of the data (in the 2000-10000 km nucleus distance range) with a dust dynamical model indicate that the grain size distribution index was of about -2.6, that the density of dust particles was very low, of about 100 kg m^{-3}, and that their geometric albedo was about 4%, suggesting the dust particles to be both very fluffy and dark (Fulle *et al.*, 2000). Rocky and carbonaceous materials were mixed together on a very fine scale and isotopic abundances appeared to be solar (Jessberger, 1999).

3.1.2 81P/Wild 2 flyby: Dust Sample Collection

Stardust collected about 4 mg of cometary material from comet 81P/Wild 2 in January 2004, capturing dust particles ejected into the coma using aerogel, with a comet-spacecraft relative speed of 6.1 km s^{-1}. After delivery of the samples to Earth in January 2006, continued analyses provided valuable insights into the properties and composition of solid cometary material. Dust impact data gathered (by DFMI) during the flyby indicated that dust particles were fragile aggregates fragmenting as they were evolving in the inner coma of the comet (Tuzzolino *et al.*, 2004). Chemical composition (from the CIDA dust mass spectrometer) indicated the predominance of organic matter with light elements present as gas phases, whereas the dust was rich in nitrogen-containing species, with the presence of some sulfur ions (Kissel *et al.*, 2004).

Analysis of the Stardust aerogels tracks showed the typical size range of dust particles to be between 5 and 25 μm. These particles are a mixture of compact and cohesive grains (65%) and friable less cohesive aggregated structures (35%) with constituent grains of a size less than 1 μm and a size distribution consistent with the ones derived in the comae of comets (Hörz *et al.*, 2006). The collected particles are chemically heterogeneous at the largest scale (of the order of 1 μm). The mean elemental composition suggests a CI-like composition consistent with a bulk solar system composition for

primitive material (e.g., Brownlee *et al.* 2012). The majority of the Stardust particles appear primarily composed of ferromagnesian silicates with a larger range of Mg-Fe content than other comets (Zolensky *et al.*, 2008), Fe-Ni sulphides and Fe-Ni metal. The range of olivine and low-Ca pyroxene compositions indicates a wide range of formation conditions, reflecting a large scale mixing between the inner and outer protoplanetary disk (Zolensky *et al.*, 2006). No hydrous phases of silicates were detected, which suggests a lack of aqueous processing of Wild 2 dust (Keller *et al.*, 2006; Zolensky *et al.*, 2011). Mg-carbonates were detected in Stardust samples, and they may be produced by large KBO collisions or by nebular condensates (Flynn *et al.*, 2008). The material accreted includes Al-rich and Si-rich chondrule fragments together with some CAI-like fragments. These materials, combined with fine-grained components in the tracks, are analogous to components in unequilibrated chondrite meteorites and clustered interplanetary dust particles collected in Earth's stratosphere, so-called "IDPs" (Joswiak *et al.*, 2012).

Organics found in comet 81P/Wild 2 dust samples show a heterogeneous and unequilibrated distribution in abundance and composition. Their characterization suggests that amorphous carbon and organic carbon are dominant (Matrajt *et al.*, 2008). The carbon isotopic composition of glycine strongly favors an non-terrestrial origin for this compound (i.e. not contamination), making it the first amino acid detected in cometary material (Elsila *et al.*, 2009).

H, C, N and O isotopic compositions are heterogeneous in the samples, but extreme anomalies are rare, indicating that Wild 2 is not a pristine aggregate of presolar materials. Few grains with ^{17}O and ^{16}O isotopic anomalies were found, showing them to be a minor phase of the comet, and indicating the presence of both presolar material and material formed at high temperature in the inner solar system and transported to the Kuiper belt before comet accretion (McKeegan *et al.*, 2006). The presence of deuterium and ^{15}N excesses also suggests that some organics have an interstellar/protostellar heritage (Sandford *et al.*, 2006). The oxygen isotopic compositions are consistent with chondritic material trends and the presence of one additional ^{16}O enriched reservoir (Nakashima *et al.*, 2012). The ^{26}Al-^{26}Mg isotope presents no evidence of radiogenic ^{26}Mg, thus indicating that part of the cometary grains have formed more than 1.7 million years after the oldest solids in the solar system, the calcium- and aluminum-rich inclusions (CAIs). This material must have been incorporated into the comet several million years after the CAIs formed (Matzel *et al.* 2010). One particular Wild 2 chondrule-like fragment, called Iris, is similar to CR chondrite materials, and was age-dated to more than 1.8 million years after CAI formation (Ogliore *et al.*, 2012). Ogliore *et al.* concluded that comet formation probably occurred after Jupiter formation and about 2 million years after CAIs.

It nevertheless needs to be noted that, due to the fragility of the dust particles and the relatively high speed of collection by Stardust, the analyses of the composition of the particles and their interpretation is perturbed by the mode of collection, which

induced partial melting of some of the material (e.g., preferential loss of light elements combined with possible amorphization and graphitization, Spencer and Zare, 2007; Fries *et al.*, 2009).

3.1.3 9P/Tempel 1 and 103P/Hartley 2: Icy Grains and Aggregates

The nucleus of comet 9P/Tempel 1 was hit in July 2005 by a projectile released by the Deep Impact spacecraft (A'Hearn *et al.*, 2005). It allowed comparison of the properties of materials found in the coma, possibly originating from a processed surface, to sub-surface materials released by the impact. After the impact, there was an enhanced UV scattering that persisted for about 20 minutes. Strong absorptions in IR spectra near 3 μm were noticed, providing evidence for icy grains in the plume (Schulz *et al.*, 2006; Sunshine *et al.*, 2007). Before impact, the C_2H_6/H_2O ratio in the coma was depleted by a factor of three relative to organics-normal comets but after impact it increased to the organics-normal value (0.6hypervolatile ethane was more depleted in the surface layer than in the excavated material (Mumma et al. 2005).

The Deep Impact spacecraft was retargeted to comet 103P/Hartley 2, which it flew by in November 2010 as part of the EPOXI mission. The nucleus was discovered to be bi-lobed in shape, with knobby terrains on the lobes and relatively smooth regions on the waist, to have an average geometric albedo of about 4%, and to present a clustering of jets on parts of the lobes (A'Hearn et al., 2011). At closest approach, many images suggested the presence of large chunks of icy particles, with sizes possibly reaching tens of centimeters. Further analyses confirmed the existence of such aggregates, sublimating on their sunny side and presenting densities below 100 kg m^{-3} (Kelley *et al.*, 2013). The velocity of the individual icy grains is smaller than the expansion velocities expected for 1 μm pure water ice particles, confirming that they are probably components of aggregates (Protopapa *et al.*, 2014).

Similarities between the material excavated from Tempel 1 and the outgassing from Hartley 2 suggest icy aggregates built of relatively pure icy grains with sizes of about one micron. Quite comparable values are also derived for near-infrared remote observations of the coma of comet 17P/Holmes after its October 2007 outburst, with solid particles in the coma suggested to consist of both refractory dust and cold ice grains, not in thermal contact (Yang *et al.*, 2009; Beer *et al.*, 2009).

3.2 Results from Remote Observations

Solid particles in cometary comae have been studied for several tens of comets bright enough to be observed from Earth or near-Earth-based observatories. Results stem

from infrared spectroscopic observations (in the 8–13 μm atmospheric window or over a larger range from space observatories), as well as from linear polarimetric observations (including polarimeric imaging techniques). After the results from Halley flybys and before space missions to JFCs, the very active Oort cloud comet C/1995 O1 (Hale-Bopp) increased our understanding of the composition of the solid component of comae. Its activity was higher than for all other comets previously observed, and significant similarities in the IR dust spectrum were found with comet Halley (Figure 7; Hanner, 1999).

3.2.1 Infrared Spectroscopy: Silicates

Silicate components of the dust contribute to a weak continuum emission and strong resonances in the 10 μm domain for Hale-Bopp. Different silicates were identified in spectra: amorphous pyroxene, amorphous olivine and crystalline olivine. Closer to the Sun, Mg-rich crystalline pyroxene was also identified. The very significant strength observed for the features in C/1995 O1 (Hale-Bopp) could be due to a large number of submicron-sized grains (0.2 μm or smaller). The smaller Mg-rich crystals could come from the jets, although no differences in silicate mineralogy were observed between the different regions, e.g., inner coma, coma and jets (Hayward *et al.*, 2000). Other Oort cloud comets present similar spectra with Mg-rich grains (Hanner, 1999; Wooden *et al.*, 2004), but with lower strength of the features.

Comet 9P/Tempel 1 was extensively observed before and after the Deep Impact event. Before impact, spectra contained a broad feature in the 8-12 μm range, attributed to amorphous silicates. Spectra of JFCs with low dust production rates are generally found to have weak silicate features, discernible in high signal-to-noise Spitzer IRS spectra of comets (Kelley and Wooden, 2009). These weak silicate features, attributable to the coma dust population, are better revealed after subtraction of the relatively strong thermal contribution from the nucleus (Hanner 1999; Sitko *et al.*, 2004; Harker *et al.*, 2005; Harker *et al.*, 2007; Kelley and Wooden, 2009; Woodward *et al.*, 2011). Weak silicate features arise from a deficiency of small grains rather than a lack of silicate material (Hanner 1999; Woodward *et al.*, 2011) *et al.*, 2005; Kelley and Wooden). After impact on Tempel 1, spectra showed a very significant feature due to crystalline Mg-silicate (see Figure 7), similar to those observed for Hale-Bopp (Harker *et al.*, 2005; 2007; Lisse *et al.*, 2007). These features progressively disappeared as the plume dissipated away from the nucleus. Grains first ejected from Tempel 1 were mainly submicron-sized amorphous-carbon grains and submicron-sized silicates (Sugita *et al.*, 2005; Harker *et al.*, 2007). The second part of the ejecta mainly contained Mg-rich crystal silicates with submicron sizes, originating in the sub-surface layer. It may be added that hydrated minerals, which have implications for the location of their formation region (Lisse *et al.*, 2007; Kelley and Wooden, 2009) have also been detected. Amorphous carbon (submicron-sized)

grains were suggested to come from a carbonaceous layer formed by cosmic irradiation during the extremely long time spent by the nucleus in the transneptunian region (Sugita *et al.*, 2007; Furusho *et al.*, 2007). This hypothesis is compatible with the observations of the impact crater by the Stardust-NExT mission (Schultz *et al.*, 2013).

Both Tempel 1 and Hale-Bopp have high-crystalline silicate fractions, but there are important differences in their precise mineralogy (Lisse *et al.*, 2007; Kelley and Wooden, 2009). In comet Hale-Bopp and many Oort cloud comets, only Mg-rich grains are present. Mg-Fe crystals are also found in Tempel 1 and JFCs. The presence of Mg-silicates requires significant processing in the protosolar nebula (Wooden *et al.*, 2002). Annealing by heating may be an important process to convert amorphous grains to crystals. New observations and modeling are necessary to understand the transport and formation of the different classes of comets.

3.2.2 Infrared Spectroscopy: Organics and Icy Particles

Refractory organics, which mainly contribute to the featureless emission and possibly to a 3.4 μm emission (Green *et al.*, 1992), are more difficult to detect. They can be mixed with rocky components, and constitute a matrix gluing the different minerals, as in IDPs (Flynn *et al.*, 2003, 2013; Flynn, 2011). They can also coat the dust grains, a process possibly having taken place in the interstellar medium (Hanner and Bradley, 2004; Greenberg and Hage, 1990; Ehrenfreund *et al.*, 2004). When particles are ejected in the coma, they get heated, leading to changes in their optical properties and even to evaporation and destruction. Distributed sources may appear (Bockeléee-Morvan *et al.*, 2004; Cottin *et al.*, 2004) and fragmentation of dust particles is likely to occur.

Remote detection of water ice is extremely difficult, with an icy grain halo likely to be limited to a few hundred kilometers at heliocentric distances below 2.5 au (Hanner, 1981, Beer *et al.*, 2006, 2008), meaning that high spatial resolution is required to attempt any detection. Water ice has three absorption bands in the near-infrared, centered at 1.5, 2.0, and 3.0 μm. First detections of water ice were obtained on comet Hale-Bopp from the UKIRT telescope with the comet at about 7 au from the Sun (Davies *et al.*, 1997) and from the ISO space observatory at 2.9 au (Lellouch *et al.* 1998). Infrared spectra of comets Hale-Bopp and C/2002 T7 (LINEAR) were reproduced with an intimate mixture of water ice and silicate spherical grains, assuming water ice to be in an amorphous state (Davies *et al.*, 1997; Kawakita *et al.*, 2004). In the infrared spectra of comets 17P/Holmes in its outburst and C/2011 L4 (PanSTARRS), water ice bands were detected at 2.0 μm and reproduced with submicron icy grains (Yang et al., 2009; 2014). Remote observations of Tempel 1 from the XMM-Newton observatory provided evidence for ice particles in the inner coma after the impact (Schulz *et al.*, 2006). Observations of color changes after the Deep Impact encounter in the visible and near IR domains also suggested an

increase in small grains and in ice relative to refractory dust in the coma (Knight *et al.*, 2007; Schleicher *et al.*, 2006). Indeed, remote observations from the Spitzer observatory suggested a very high ice-to-dust ratio of about 10 in the excavated material (which greatly exceeds the gas-to-dust production rate ratio of about 0.5 measured for the background coma), although a ratio in the 1 to 3 range cannot be excluded if a large amount of material fell back to the surface and sublimated (Gicquel *et al.*, 2012).

3.2.3 Color and Polarimetric (Linear and Circular) Observations

Observations of solar light scattered by solid particles in cometary comae depend on the observational conditions (e.g., phase angle, wavelength) and on the particles' physical properties (e.g., complex refractive indices and composition, size, shape, geometric albedo). Differences in physical properties between the particles in different regions of the coma are pointed out by differences in the linear polarization of the scattered light and by spectral variations in brightness and polarization. At visible wavelengths, grains or particles with sizes of between 0.5 and 10 μm seem to dominate the scattered light, affecting the degree of linear polarization and color variation in the brightness and in the polarization.

The color of the dust is associated with the variation of the scattered intensity with wavelength. In the visible domain, the scattered light is generally redder than the solar continuum (Jewitt and Meech, 1986; Kolokolova *et al.*, 2004). The reddening slope decreases towards the near-infrared. The color depends on the size distribution of the grains and aggregates and on their refractive indices, mainly for grains larger than the wavelength. Some local variations of colors have been observed in comae. In comet Hale-Bopp, the color in the curved jets was less red than the average background, possibly because of an increase in the number of submicron-sized grains (Furusho *et al.*, 1999). At the beginning of the disruption of comet C/1999 S4 (LINEAR), the color was bluer while fast moving small grains were detected, although the color of the largest fragments was red and became less red when the fragmenting particles went farther away from the nucleus (e.g., Hadamcik and Levasseur-Regourd, 2003a). To interpret the slightly bluer color in the visible and near infrared in the dust ejecta after the Deep Impact event, small submicron-sized grains were suggested, as well as the presence of pure or mixed water ice crystals or the sublimation of organics (Hodapp *et al.*, 2007; Fernandez *et al.*, 2007; Beer *et al.*, 2009). Generally, bluer color requires relatively transparent grain materials such as water ice, Mg-rich silicates, or perhaps non-radiation damaged nor heated organics (Kiselev *et al.*, 2004: Hadamcik and Levasseur-Regourd, 2009; Zubko *et al.*, 2011, 2012; Hadamcik *et al.*, 2014).

The solar light scattered by cometary comae is partially linearly polarized. Polarimetric properties vary with size and size distribution, morphology and structure, as

well as with complex refractive indices, of the scattering particles. Observations can thus point out changes in dust properties and provide information on composition through numerical and experimental simulations (see e.g. for reviews, Kolokolova *et al.*, 2015). Evidence for changes in local polarization was established by OPE/Giotto during the Halley flyby, with an increase in jets and a decrease near the nucleus at constant large phase angle and wavelength (Levasseur-Regourd *et al.* 1999). Such behavior could also be monitored by remote CCD imaging polarimery on comet Levy (Renard *et al.*, 1992) and later on other comets at different phase angles (e.g., Jones and Gehrz, 2000; Hadamcik and Levasseur-Regourd, 2003b, Hadamcik *et al.*, 2013; Deb Roy *et al.*, 2015; Hines *et al.*, 2014).

Three main regions of polarization have been detected, as illustrated in Figure 8: the background coma, jet-like features (in active comets) with a higher polarization than in the coma, and (for some comets only) a circumnucleus polarimetric halo, clearly detected on polarimetric images of comets Levy and Hale-Bopp at different phase angles. The polarization in the halo, if any, is more negative than the surroundings for phase angles smaller than about 20° (see Fig. 8, a and b) and is lower than the surrounding coma for larger phase angles (see Fig. 8, c and d).

The averaged polarization, measured through different increasing aperture sizes (e.g., Kiselev *et al.*, 2001; Hadamcik *et al.*, 2013), provides the whole coma polarization when using large apertures (Hadamcik and Levasseur-Regourd, 2003b), for a given phase angle and wavelength. Polarimetric phase curves show a small negative branch (down to about -1 to -2%), and inversion angle near 20°, and a broad positive branch with a maximum (up to about 15 to 30%) by 90° to 100° (e.g. Hadamcik and Levasseur-Regourd, 2003b). From synthetic phase curves built for all observed comets in the same wavelength range, two classes may be characterized (see Figure 9): the active comets with generally well focused jets that present a high maximum in polarization, and the comets that present a lower maximum in polarization (Levasseur-Regourd *et al.*, 1996). The latter are less active or may show an important decrease of polarization away from the photometric center, such as comet Tempel 1 before the Deep Impact event (Hadamcik *et al.*, 2007a) or comet C/1996 Q1 (Tabur) (Kiselev *et al.*, 2001).

For a given phase angle above 20°, the whole coma polarization slightly increases with the wavelength, at least up to about 2 μm. It seems to decrease for wavelengths greater than 2 μm, possibly due to some thermal emission (Kolokolova *et al.*, 2004), although observations and thermal models of cometary comae show that the thermal emission has its onset between 3 μm and 4 μm for heliocentric distances in the 1–3 AU range (Sitko *et al.*, 2004; Harker *et al.*, 2002, 2004). A decrease of polarization with increasing wavelength in the visible has been observed for some comets such as 21P/Giacobini-Zinner (Kiselev *et al.*, 2000) or during some event such as the complete disruption of comet C/1999 S4 (LINEAR) (Hadamcik *et al.*, 2003a). In the circumnucleus polarimetric halo region, such a spectral gradient inversion was noticed through *in situ* observations

of Halley and remote observations of Hale-Bopp, possibly providing clues to different properties for freshly ejected dust particles.

In addition to its linear polarization, the light scattered by cometary dust appears to present a weak circular polarization signal. The origin of circular polarization is still debated but could arise from the alignment of dust particles, light scattering by asymmetric particles, or the presence of prebiotic homochiral organic molecules in cometary dust. More observations are necessary to better constrain its origin. A discussion can be found in Kiselev *et al.*, 2014.

3.2.4 Properties of Solid Particles Inferred from Light Scattering Measurements, with Emphasis on Composition

Numerous authors have tried to constrain the scattering properties of cometary dust. From experimental simulations, Hadamcik *et al.* (2007b) established that fluffy Mg-Fe-SiO and C mixtures could represent satisfactory cometary dust analogs. From numerical simulations of polarization data and silicate emission features, Kolokolova *et al.* (2007) concluded that the dust in comets with a high maximum in polarization consists of highly porous aggregates that may be associated with fresh dust as in new comets. The dust in comets with a lower maximum polarization consists of less porous particles which may be associated with more highly processed dust such as expected for the surfaces of JFC comets. Compact porous particles also dominated the coma of long period comet C/2007 N3 (Lulin), as evidenced by a negative branch that extended to near-IR wavelengths (Woodword *et al.*, 2011). Finally, whenever polarimetric phase curves are obtained on a large enough range of phase angles in different wavelengths (as possible mostly for Halley and Hale-Bopp), numerical and experimental simulations may be used to infer some average properties, such as size and size distribution, ratio between transparent and absorbing materials, and ratio between fluffy aggregates and compact particles (Levasseur-Regourd *et al.*, 2008; Lasue *et al.*, 2009; Zubko *et al.*, 2012; Hines *et al.*, 2014).

The circumnucleus polarimetric halo provides an example of the complexity of interpretations. First of all, it is not always observed; it can be hidden by jets or not continuously present or may not exist at all. Secondly, its interpretation is controversial. The deep negative branches observed for C/1995 O1 (Hale-Bopp) and 81P/Wild 2 seem to be possible only if transparent particles exist in this region. Suggestions are large agglomerates of water ice grains, an excess of Mg-rich silicate grains as compared to dark carbonaceous compounds, and relatively transparent organics, possibly covering silicate grains (Flynn *et al.*, 2003; Flynn *et al.*, 2013). These organics, heated in the coma after ejection, may become darker by carbonization and can release gases as an extended source (Hadamcik *et al.*, 2014). Various compositions and evolutions may actually co-exist in the innermost comae. Additionally, a smaller polarization may originate in some

depolarization induced by multiple scattering, as was certainly the case in the plume ejected from Tempel 1 after impact. Nevertheless, the polarimetric spectral gradient, possibly negative or neutral near the nucleus, and positive after an evolution of the composition, could provide further clues.

There can be a strong synergy between the dust particle properties derived from studies of color and linear polarization with their properties assessed by studies of coma dynamics and thermal emission, where comet Hale-Bopp is an excellent example. As stated in subsection 3.2.3, Hale-Bopps curved jets or arcs were less red than the average background, possibly because of an increase in the number of submicron-sized grains. Compared to the background coma, Hale-Bopp arcs also showed higher linear polarization (Jones and Gehrz, 2000), higher dust color temperatures (Hayward et al., 2000), strong silicate features (Hayward et al., 2000) indicative of a high concentration of submicron silicate crystals as well as micron-sized porous particles (Harker et al., 2002, 2004). The coma dynamical models showed that arc/jet particles needed to be small (submicron) and relatively transparent in order that solar radiation pressure not smear out the arcs nor compress the arc spacing (Hayward et al., 2000). Ground truth, as expected from a rendezvous mission such as Rosetta, monitoring the dust properties of a given comet at different distances from the nucleus and from the Sun, coupled with remote observations, is certainly of major importance for future interpretations of spectroscopic and polarimetric observations of various comets.

3.3 Sun-Grazing Comets

When a comet gets very close to the Sun, it is heated sufficiently that the refractory particles can start to sublimate, releasing metals such as Na and K in the coma. Observations of these metals can give key insights into the atomic abundances in cometary dust that can only otherwise be gleaned with dust analyzers *in situ*. However, these lines only become prominent when a comet is very close to the Sun, challenging our ability to observe the comet from the ground or with space telescopes owing to the small solar elongation. Indeed, these comets are so close to the Sun that the observations must be obtained during the daytime. As noted above, comet C/2012 S1 (ISON) was one such Sun-grazing comet that was extensively observed, though it faded substantially when closest to the Sun, limiting our ability to detect the metal lines.

Comet C/1965 S1 (Ikeya-Seki) was one of the brightest Sun-grazing comets to be studied spectroscopically. Observations were obtained from Kitt Peak National Observatory (Slaughter, 1969; Arpigny, 1979), Lick Observatory (Preston, 1967), Sacramento Peak (Curtis, 1966), Haute Provence (Dufay *et al.*, 1965), Radcliffe (Thackeray *et al.*, 1966), and possibly others, when the comet was as close to the Sun as ~ 14 solar radii.

In addition to the normal cometary gas emissions, emission lines due to Na I, K I,

Ca I, Ca II, Cr I, Mn I, Fe I, Ni I, Cu I, Co I, and V I were observed. From analysis of the Fe lines, a Boltzmann temperature of $\sim 4500\,K$ was determined (Slaughter, 1969; Preston, 1967). Arpigny (1979) noted that Mg, Al, Si ad Ti were not detected. Compared with solar abundances, the abundances of some of these metals were underabundant, while others were overabundant (Arpigny, 1979; Preston, 1967). However, arguments were presented (Arpigny, 1979) that the relative *elemental* abundances were probably close to solar or meteoritic values.

3.4 Dust Composition: Rosetta Capabilities and Early Results

The instruments on the Rosetta mission that could provide direct information on the composition of solid particles for 67P/Churyumov-Gerasimenko (CG) are mostly COSIMA and VIRTIS on the main Rosetta spacecraft, to be used during the whole rendezvous mission, and COSAC at Philae landing. The COmetary Secondary Ion Mass Analyser, COSIMA, is the first instrument applying SIMS (secondary ion mass spectrometry) technique to *in situ* analysis. It collects dust particles at the Rosetta location on targets handled by a manipulation unit, in order to obtain time-of-flight spectra over a mass range from 1 to 3500 amu, leading to the composition of the dust particles, whether they are organic or inorganic (Kissel *et al.*, 2007). The Visual IR Thermal Imaging Spectrometer, VIRTIS, provides imaging spectroscopy in the 0.25-5.0 μm spectral range, in order to map composition and evolution of dust jets in the coma, as well as to derive the composition of the dust grains in the inner coma and on the surface (Coradini *et al.*, 2007). By August 2014, strong hints of carbon-bearing compounds, with spectral features compatible with complex macromolecular carbonaceous materials, were already noted on the nucleus surface. (http://blogs.esa.int/rosetta/2014/09/08/virtis-maps-comet-hot-spots/). The COmetary SAmpling and Composition experiment, COSAC, relies on a multi-column enantio-selective gas chromatograph, coupled to a linear time-of-flight mass spectrometer to derive the composition of volatile species collected at the surface and at about 20 cm below the surface with the Philae lander (Goesmann *et al.*, 2007).

Interpretation of data, e.g., from dust experiments GIADA (Colangeli *et al.*, 2007), COSIMA (Kissel *et al.*, 2007) and MIDAS (Riedler *et al.*, 2007) on Rosetta, as well as from CONSERT (Kofmann *et al.*, 2007), APSX (Klingelhöfer *et al.*, 2007) or Ptolemy (Wright *et al.* 2007) on Philae, should also significantly contribute to a better understanding of the dust composition, and on its evolution i) from the subsurface to the surface of the nucleus and to the coma and ii) from large and decreasing solar distances before perihelion passage to increasing solar distances after perihelion passage.

Preliminary results from the Rosetta mission have already established that the surface of CG is rich in non-volatile organics, likely complex mixtures of various carbon-hydrogen (aromatic and aliphatic), oxygen-hydrogen (carboxylic or alcoholic) and nitrogen-hydrogen groups (Capaccioni *et al.*, 2015). The largest particles (with sizes greater

than 50 μm) are demonstrated to be fluffy and fragile aggregates, and found to present sodium-rich surfaces (Schulz *et al.*, 2015). While the presence of such aggregates had been suspected from simulations (e.g., Hadamcik et al., 2007a; Levasseur-Regourd et al., 2008), the Rosetta ground-truth now allows us to speculate about the early Solar System evolution. A significant amount of non-volatile organics could have enriched the surface of terrestrial planets, with fluffy particles more resistant to atmospheric ablation than compact ones. More results and discoveries are soon expected, from Rosetta pre-perihelion (at solar distances less than 3 AU) and post-perihelion measurements, and from Philae measurements.

4 Summary

We have learned a great deal about comets from the studies outlined in this paper. However, the picture is not yet fully coherent since we find different stories when we change wavelength. The Rosetta mission will help us to gain detail and to compare with the data that have come before. However, it is obvious that all that can be learned from the enigmatic comets has not yet been found.

Acknowledgements: The authors would like to thank Dr. Paul Feldman, Dr. Jacques Crovisier, Dr. Neil Dello Russo and Dr. Adam McKay for helpful comments and making data available for our use. Partial support from CNES (the French spatial agency) is acknowledged.

References

A'Hearn, M. F., M. J. S. Belton, W. A. Delamere, L. M. Feaga, D. Hampton, J. Kissel, K. P. Klaasen, L. A. McFadden, K. J. Meech, H. J. Melosh, P. H. Schultz, J. M. Sunshine, P. C. Thomas, J. Veverka, D. D. Wellnitz, D. K. Yeomans, S. Besse, D. Bodewits, T. J. Bowling, B. T. Carcich, S. M. Collins, T. L. Farnham, O. Groussin, B. Hermalyn, M. S. Kelley, M. S. Kelley, J.-Y. Li, D. J. Lindler, C. M. Lisse, S. A. McLaughlin, F. Merlin, S. Protopapa, J. E. Richardson, and J. L. Williams 2011. EPOXI at comet Hartley 2. *Science* **332**, 1396–1400.

A'Hearn, M. F., M. J. S. Belton, W. A. Delamere, J. Kissel, K. P. Klaasen, L. A. McFadden, K. J. Meech, H. J. Melosh, P. H. Schultz, J. M. Sunshine, P. C. Thomas, J. Veverka, D. K. Yeomans, M. W. Baca, I. Busko, C. J. Crockett, S. M. Collins, M. Desnoyer, C. A. Eberhardy, C. M. Ernst, T. L. Farnham, L. Feaga, O. Groussin, D. Hampton, S. I. Ipatov, J.-Y. Li, D. Lindler, C. M. Lisse, N. Mastrodemos, W. M. Owen, J. E. Richardson, D. D. Wellnitz, and R. L. White 2005. Deep Impact: Excavating Comet Tempel 1. *Science* **310**, 258–264.

A'Hearn, M. F. and R. L. Millis 1980. Abundance correlations among comets. *A. J.* **85**, 1528–1537.

A'Hearn, M. F., R. L. Millis, D. G. Schleicher, D. J. Osip, and P. V. Birch 1995. The ensemble properties of comets: Results from narrowband photometry of 85 comets, 1976–1992. *Icarus* **118**, 223–270.

Altwegg, K., H. Balsiger, A. Bar-Nun, J. J. Berthelier, A. Bieler, P. Bochsler, C. Briois, U. Calmonte, M. Combi, J. De Keyser, P. Eberhardt, B. Fiethe, S. Fuselier, S. Gasc, T. I. Gombosi, K. C. Hansen, M. Hässig, A. Jäckel, E. Kopp, A. Korth, L. LeRoy, U. Mall, B. Marty, O. Mousis, E. Neefs, T. Owen, H. Rème, M. Rubin, T. Sémon, C.-Y. Tzou, H. Waite, and P. Wurz 2015. 67P/Churyumov-Gerasimenko, a Jupiter family comet with a high D/H ratio. *Science* **347**, A387.

Arpigny, C. 1979. Relative abundances of the heavy elements in comet Ikeya-Seki (1965 VIII). In *Liege International Astrophysical Colloquia* (A. Boury, N. Grevesse, and L. Remy-Battiau, Eds.) pp. 189–197.

Arpigny, C., E. Jehin, J. Manfroid, D. Hutsemékers, R. Schulz, J. A. Stüwe, J.-M. Zucconi, and I. Ilyin 2003. "Anomalous" nitrogen isotope ratio in comets. *Science* **301**, 1522–1524.

Balsiger, H., K. Altwegg, P. Bochsler, P. Eberhardt, J. Fischer, S. Graf, A. Jäckel, E. Kopp, U. Langer, M. Mildner, J. Müller,

T. Riesen, M. Rubin, S. Scherer, P. Wurz, S. Wüthrich, E. Arijs, S. Delanoye, J. de Keyser, E. Neefs, D. Nevejans, H. Rème, C. Aoustin, C. Mazelle, J.-L. Médale, J. A. Sauvaud, J.-J. Berthelier, J.-L. Bertaux, L. Duvet, J.-M. Illiano, S. A. Fuselier, A. G. Ghielmetti, T. Magoncelli, E. G. Shelley, A. Korth, K. Heerlein, H. Lauche, S. Livi, A. Loose, U. Mall, B. Wilken, F. Gliem, B. Fiethe, T. I. Gombosi, B. Block, G. R. Carignan, L. A. Fisk, J. H. Waite, D. T. Young, and H. Wollnik 2007. Rosina-Rosetta Orbiter Spectrometer for Ion and Neutral Analysis. *Space Science Rev.* **128**, 745–801.

Balsiger, H., K. Altwegg, and J. Geiss 1995. D/H and $^{18}O/^{16}O$ ratio in the hyronium ion and in neutral water from *in situ* ion measurements in comet 1P/Halley. *J. Geophys. Res.* **100**, 5827–5834.

Beer, E., M. Podolak, and D. Prialnik 2006. The contribution of icy grains to the activity of comets. I. Grains lifetime and distribution. *Icarus* **180**, 473–486.

Beer, E., D. Prialnik, and M. Podolak 2008. The contribution of grains to the activity of comets. II. The brightness of the coma. *Icarus* **195**, 340–347.

Beer, E., D. H. Wooden, and R. Schulz 2009. The grain evolution model for icy grains ejected from 9P/Tempel 1 by Deep Impact. In *Deep Impact as a World Observatory Event: Synergies in Space, Time and Wavelengths* (H. U. Kaüfl and C. Sterken, Eds.) pp. 59–67 Springer.

Biver, N., D. Bockel'ee-Morvan, P. Colom, J. Crovisier, J. K. Davies, W. R. F. Dent, D. Despois, E. Gerard, E. Lellouch, H. Rauer, R. Moreno, and G. Paubert 1997. Evolution of the outgassing of comet Hale-Bopp (C/1995 O1) from radio observations. *Science* **275**, 1915–1918.

Biver, N., D. Bockelée-Morvan, P. Colom, J. Crovisier, F. Henry, E. Lellouch, A. Winnberg, L. E. B. Johansson, M. Gunnarsson, H. Rickman, F. Rantakyrö, J. K. Davies, W. R. F. Dent, G. Paubert, R. Moreno, J. Wink, D. Despois, D. J. Benford, M. Gardner, D. C. Lis, D. Mehringer, T. G. Phillips, and H. Rauer 2002. The 1995–2002 long-term monitoring of comet C/1995 O1 (Hale-Bopp) at radio wavelength. *Earth, Moon, Planets* **90**, 5–14.

Blake, G. A., C. Qi, M. R. Hogerheijde, M. A. Gurwell, and D. O. Muhleman 1999. Sublimation from icy jets as a probe of the interstellar volatile content of comets. *Nature* **398**, 213–216.

Bockelée-Morvan, D. 2011. An overview of comet composition. In *IAU Symposium 280* (J. Cernicharo and R. Bachiller, Eds.) pp. 261–274.

Bockelée-Morvan, D., J. Crovisier, M. J. Mumma, and H. A. Weaver 2004. The composition of cometary volatiles. In *Comets II* (M. C. Festou, H. U. Keller, and H. A. Weaver, Eds.) p. 391 Univ. of Arizona Press Tucson, AZ.

Bockelée-Morvan, D., D. C. Lis, J. E. Wink, D. Despois, J. Crovisier, R. Bachiller, D. J. Benford, N. Biver, P. Colom, J. K. Davies, E. Gérard, B. Germain, M. Houde, D. Mehringer, R. Moreno, G. Paubert, T. G. Phillips, and H. Rauer 2000. New molecules found in comet C/1995 O1 (Hale-Bopp). Investigating the link between cometary and interstellar material. *Astr. and Ap.* **353**, 1101–1114.

Boissier, J., D. Bockelée-Morvan, N. Biver, P. Colom, J. Crovisier, R. Moreno, V. Zakharov, O. Groussin, L. Jorda, and D. C. Lis 2014. Gas and dust productions of comet 103P/Hartley 2 from millimetre observations: Interpreting rotation-induced time variations. *Icarus* **228**, 197–216.

Boissier, J., D. Bockelée-Morvan, N. Biver, J. Crovisier, D. Despois, B. G. Marsden, and R. Moreno 2007. Interferometric imaging of the sulfur-bearing molecules H_2S, SO, and CS in comet C/1995 O1 (Hale-Bopp). *Astr. and Ap.* **475**, 1131–1144.

Bonev, B. P., M. A. DiSanti, G. L. Villanueva, E. L. Gibb, L. Paganini, and M. J. Mumma 2014. The inner coma of comet C/2012 S1 (ISON) at 0.53 AU and 0.35 AU from the Sun. *Ap. J.* **796**, L6.

Bonev, B. P., M. J. Mumma, Y. L. Radeva, M. A. DiSanti, E. L. Gibb, and G. L. Villanueva 2008. The peculiar volatile composition of comet 8P/Tuttle: A contact binary of chemically distinct cometesimals? *Ap. J.* **680**, L61–L64.

Bonev, B. P., G. L. Villanueva, L. Paganini, M. A. DiSanti, E. L. Gibb, J. V. Keane, K. J. Meech, and M. J. Mumma 2013. Evidence for two modes of water release in comet 103P/Hartley 2: Distributions of column density, rotational temperature, and ortho-para ratio. *Icarus* **222**, 740–751.

Brownlee, D., D. Joswiaka, and G. Matrajt 2012. Overview of the rocky component of Wild 2 comet samples: Insight into the early solar system, relationship with meteoritic materials and the differences between comets and asteroids. *Meteoritics Planet. Sci.* **47**, 453–470.

Capaccioni, F., A. Coradini, G. Filacchione, S. Erard, G. Arnold, P. Drossart, M. C. De Sanctis, D. Bockelee-Morvan, M. T. Capria, F. Tosi, C. Leyrat, B. Schmitt, E. Quirico, P. Cerroni, V. Mennella, A. Raponi, M. Ciarniello, T. McCord, L. Moroz, E. Palomba, E. Ammannito, M. A. Barucci, G. Bellucci, J. Benkhoff, J. P. Bibring, A. Blanco, M. Blecka, R. Carlson, U. Carsenty, L. Colangeli,

M. Combes, M. Combi, J. Crovisier, T. Encrenaz, C. Federico, U. Fink, S. Fonti, W. H. Ip, P. Irwin, R. Jaumann, E. Kuehrt, Y. Langevin, G. Magni, S. Mottola, V. Orofino, P. Palumbo, G. Piccioni, U. Schade, F. Taylor, D. Tiphene, G. P. Tozzi, P. Beck, N. Biver, L. Bonal, J.-P. Combe, D. Despan, E. Flamini, S. Fornasier, A. Frigeri, D. Grassi, M. Gudipati, A. Longobardo, K. Markus, F. Merlin, R. Orosei, G. Rinaldi, K. Stephan, M. Cartacci, A. Cicchetti, S. Giuppi, Y. Hello, F. Henry, S. Jacquinod, R. Noschese, G. Peter, R. Politi, J. M. Reess, and A. Semery 2015. The organic-rich surface of comet 67P/Churyumov-Gerasimenko as seen by VIRTIS/Rosetta. *Science* **347**, 628.

Capria, M. T., G. Cremonese, A. Bhardwaj, and M. C. De Sanctis 2005. O (^{1}S) and O (^{1}D) emission lines in the spectrum of 153P/2002 C1 (Ikeya-Zhang). *Astr. and Ap.* **442**, 1121–1126.

Capria, M. T., G. Cremonese, A. Bhardwaj, M. C. De Sanctis, and E. Mazzotta Epifani 2008. Oxygen emission lines in the high resolution spectra of 9P/Tempel 1 following the Deep Impact event. *Astr. and Ap.* **479**, 257–263.

Cochran, A. L. 1987. Another look at abundance correlations among comets. *A. J.* **93**, 231–238.

Cochran, A. L. 2008. Atomic oxygen in the comae of comets. *Icarus* **198**, 181–188.

Cochran, A. L., E. S. Barker, and C. L. Gray 2012. Thirty years of cometary spectroscopy from McDonald Observatory. *Icarus* **218**, 144–168.

Cochran, A. L. and W. D. Cochran 2001. Observations of O (^{1}S) and O (^{1}D) in spectra of C/1999 S4 (LINEAR). *Icarus* **154**, 381–390.

Code, A. D., T. E. Houck, and C. F. Lillie 1972. Ultraviolet observations of comets. In *Scientific results from the orbiting astronomical observatory (OAO-2)* p. 109.

Colangeli, L., J. J. Lopez-Moreno, P. Palumbo, J. Rodriguez, M. Cosi, V. Della Corte, F. Esposito, M. Fulle, M. Herranz, J. M. Jeronimo, A. Lopez-Jimenez, E. M. Epifani, R. Morales, F. Moreno, E. Palomba, and A. Rotundi 2007. The grain impact analyser and dust accumulator (GIADA) experiment for the Rosetta Mission: Design, performances and first results. *Space Science Rev.* **128**, 803–821.

Colom, P., J. Crovisier, N. Biver, and D. Bockelée-Morvan 2011. Observations of the 18-cm lines of OH in comets with the Nançay radio telescope. In *EPSC-DPS Joint Meeting 2011* p. 837.

Combi, M. R., Z. Boyd, Y. Lee, T. S. Patel, J.-L. Bertaux, E. Quémerais, and J. T. T. Mäkinen 2011. SOHO/SWAN observations of comets with small perihelia: C/2002 V1 (NEAT), C/2002 X5 (Kudo-Fujikawa), 2006 P1 (McNaught) and 96P/Machholz 1. *Icarus* **216**, 449–461.

Combi, M. R., N. Fougere, J. T. T. Mäkinen, J.-L. Bertaux, E. Quémerais, and S. Ferron 2014. Unusual water production activity of comet C/2012 S1 (ISON): Outbursts and continuous fragmentation. *Ap. J.(Letters)* **788**, L7.

Coradini, A., F. Capaccioni, P. Drossart, G. Arnold, E. Ammannito, F. Angrilli, A. Barucci, G. Bellucci, J. Benkhoff, G. Bianchini, J. P. Bibring, M. Blecka, D. Bockelee-Morvan, M. T. Capria, R. Carlson, U. Carsenty, P. Cerroni, L. Colangeli, M. Combes, M. Combi, J. Crovisier, M. C. De Sanctis, E. T. Encrenaz, S. Erard, C. Federico, G. Filacchione, U. Fink, S. Fonti, V. Formisano, W. H. Ip, R. Jaumann, E. Kuehrt, Y. Langevin, G. Magni, T. McCord, V. Mennella, S. Mottola, G. Neukum, P. Palumbo, G. Piccioni, H. Rauer, B. Saggin, B. Schmitt, D. Tiphene, and G. Tozzi 2007. VIRTIS: An imaging spectrometer for the Rosetta Mission. *Space Science Rev.* **128**, 529–559.

Cordiner, M. A., A. J. Remijan, J. Boissier, S. N. Milam, M. J. Mumma, S. B. Charnley, L. Paganini, G. Villanueva, D. Bockelée-Morvan, Y.-J. Kuan, Y.-L. Chuang, D. C. Lis, N. Biver, J. Crovisier, D. Minniti, and I. M. Coulson 2014. Mapping the release of volatiles in the inner comae of comets C/2012 F6 (Lemmon) and C/2012 S1 (ISON) using the Atacama Large Millimeter/Submillimeter Array. *Ap. J.(Letters)* **792**, L2.

Cottin, H., M.-C. Gazeau, Y. Benilan, and F. Raulin 2004. Origin of cometary extended sources from degradation of refractory organics on grains: Polyoxymethylene as formaldehyde parent molecule. *Icarus* **167**, 397–416.

Crovisier, J., N. Biver, D. Bockelée-Morvan, J. Boissier, P. Colom, and D. C. Lis 2009. The chemical diversity of comets: Synergies between space exploration and ground-based radio observations. *Earth, Moon, Planets* **105**, 267–272.

Crovisier, J., D. Bockelée-Morvan, N. Biver, P. Colom, D. Despois, and D. C. Lis 2004. Ethylene glycol in comet C/1995 O1 (Hale-Bopp). *Astr. and Ap.* **418**, L35–L38.

Crovisier, J., P. Colom, E. Gérard, D. Bockelée-Morvan, and G. Bourgois 2002. Observations at Nançay of the OH 18-cm lines in comets. the data base. Observations made from 1982 to 1999. *Astr. and Ap.* **393**, 1053–1064.

Curtis, G. W. 1966. Daylight observations of the 1965 f comet at the Sacramento Peak Observatory. *A. J.* **71**, 194–196.

Danks, A. C., D. L. Lambert, and C. Arpigny 1974. The $^{12}C/^{13}C$ ratio in comet Kohoutek (1973f). *Ap. J.* **194**, 745–751.

Davies, J. K., T. L. Roush, D. P. Cruikshank, M. J. Bartholomew, T. R. Geballe, T. Owen, and C. de Bergh 1997. The detection of water ice in comet Hale-Bopp. *Icarus* **127**, 238–245.

Deb Roy, P., H. S. Das, and B. J. Medhi 2015. Imaging polarimetry of comet C/2012 L2. *Icarus* **245**, 241–246.

Decock, A., E. Jehin, D. Hutsemékers, and J. Manfroid 2013. Forbidden oxygen lines in comets at various heliocentric distances. *Astr. and Ap.* **555**, A34.

Decock, A., E. Jehin, P. Rousselot, D. Hutsemékers, J. Manfroid, S. Raghuram, A. Bhardwaj, and B. Hubert 2015. Forbidden oxygen lines at various nucleocentric distances in comets. *Astr. and Ap.* **573**, A1.

Dello Russo, N., M. Mumma, M. Disanti, K. Magee-Sauer, E. Gibb, B. Bonev, I. McLean, and L. Xu 2006. A high-resolution infrared spectral survey of comet C/1999 H1 Lee. *Icarus* **184**, 255–276.

Dello Russo, N., R. Vervack, H. Weaver, C. Lisse, H. Kawakita, H. Kobayashi, A. McKay, A. Cochran, W. Harris, N. Biver, D. Bockelée-Morvan, J. Crovisier, E. Jehin, and M. DiSanti 2014a. The evolving chemical composition of C/2012 S1 (ISON) as it approached the Sun. Asteroids, Comets, Meteors 2014, Helsinki, Finland.

Dello Russo, N., R. J. Vervack, H. Kawakita, H. Kobayashi, H. A. Weaver, W. M. Harris, A. Cochran, N. Biver, D. Bockelée-Morvan, and J. Crovisier 2014b. The volatile composition of 81P/Wild 2 from ground-based high-resolution infrared spectroscopy. *Icarus* **238**, 125–136.

Dello Russo, N., R. J. Vervack, H. A. Weaver, C. M. Lisse, H. Kawakita, H. Kobayashi, A. L. Cochran, W. M. Harris, D. Bockelée-Morvan, N. Biver, J. Crovisier, and A. J. McKay 2013. A high-resolution infrared spectral survey of 103P/Hartley 2 on the night of the EPOXI closest approach. *Icarus* **222**, 707–722.

DiSanti, M. A., B. P. Bonev, E. L. Gibb, G. L. Villanueva, K. J. V., L. Paganini, M. J. Mumma, G. A. Blake, A. J. McKay, and K. J. Meech 2015. En route to destruction: The composition of ices in C/2012 S1 (ISON) between 1.2 and 0.35 AU from the Sun. Submitted to the Astrophysical Journal.

DiSanti, M. A., B. P. Bonev, G. L. Villanueva, and M. J. Mumma 2013. Highly depleted ethane and mildly depleted methanol in comet 21P/Giacobini-Zinner: Application of a new empirical ν_2-band model for CH_3OH near 50 K. *Ap. J.* **763**, 1.

DiSanti, M. A., G. L. Villanueva, L. Paganini, B. P. Bonev, J. V. Keane, K. J. Meech, and M. J. Mumma 2014. Pre- and post-perihelion observations of C/2009 P1 (Garradd): Evidence for an oxygen-rich heritage? *Icarus* **228**, 167–180.

Dufay, J., P. Swings, and C. Fehrenbach 1965. Spectrographic observations of comet Ikeya-Seki (1965f). *Ap. J.* **142**, 1698.

Eberhardt, P. 1999. Comet Halley's gas composition and extended sources: Results from the neutral mass spectrometer on Giotto. *Sp. Sci. Rev.* **90**, 45–52.

Eberhardt, P., M. Reber, D. Krankowsky, and R. R. Hodges 1995. The D/H and $^{18}O/^{16}O$ ratios in water from comet P/Halley. *Astr. and Ap.* **302**, 301–316.

Ehrenfreund, P., H. J. Fraser, J. Blum, J. H. E. Cartwright, J. M. García-Ruiz, E. Hadamcik, A. C. Levasseur-Regourd, S. Price, F. Prodi, and A. Sarkissian 2003. Physics and chemistry of icy particles in the universe: Answers from microgravity. *Plan. and Space Sci.* **51**, 473–494.

Elsila, J., D. Glavin, and J. Dworkin 2009. Cometary glycine detected in samples returned by Stardust. *Meteoritics Planet. Sci.* **44**, 1323–1330.

Feldman, P. D. 2005. Spectroscopy of comets with the Far Ultraviolet Spectroscopic Explorer satellite. *Phys. Scripta* **T119**, 7–12.

Feldman, P. D., A. L. Cochran, and M. R. Combi 2004. Spectroscopic investigations of fragment species in the coma. In *Comets II* (M. C. Festou, H. U. Keller, and H. A. Weaver, Eds.) pp. 425–447 The University of Arizona Press Tucson, AZ.

Feldman, P. D., R. E. Lupu, S. R. McCandliss, and H. A. Weaver 2009. The far-ultraviolet spectral signatures of formaldehyde and carbon dioxide in comets. *Ap. J.* **699**, 1104–1112.

Fernández, Y. R., C. M. Lisse, M. S. Kelley, N. Dello Russo, A. T. Tokunaga, C. E. Woodward, and D. H. Wooden 2007. Near-infrared light curve of comet 9P/Tempel 1 during Deep Impact. *Icarus* **187**, 220–227.

Festou, M. C. 1998. 18 years of systematic UV studies of comets with IUE. In *Ultraviolet Astrophysics Beyond the IUE Final Archive* (W. Wamsteker, R. Gonzalez Riestra, and B. Harris, Eds.) pp. 45–51.

Festou, M. C. and P. D. Feldman 1981. The forbidden oxygen lines in comets. *Astr. and Ap.* **103**, 154–159.

Fillion, J.-H., M. Bertin, A. Lekic, A. Moudens, L. Philippe, and X. Michaut 2012. Understanding the relationship between gas and ice: Experimental investigations on ortho-para ratios. In *European Conference on Laboratory Astrophysics* (C. Stehlè, C. Joblin, and L. dHendecourt, Eds.) pp. 307–314.

Fink, U. 2009. A taxonomic survey of comet composition 1985 – 2004 using CCD spectroscopy. *Icarus* **201**, 311–334.

Fink, U. and M. D. Hicks 1996. A survey of 39 comets using CCD spectroscopy. *Ap. J.* **459**, 720–743.

Flynn, G. 2011. Organic grain coatings in primitive interplanetary dust: A timescale for formation of Solar System organic matter. Workshop on Formation of the first solids in the Solar System. Kauai Hawaii. LPI Contrib. 1639, p. 9143.

Flynn, G., S. Wirick, and L. P. Keller 2013. Organic grain coatings in primitive interplanetary dust particles: Implications for grain sticking in the solar nebula. *Earth Planets Space* **65**, 1159–1166.

Flynn, G. J., L. P. Keller, M. Feser, S. Wirick, and C. Jacobsen 2003. The origin of organic matter in the Solar System: Evidence from the interplanetary dust particles. *Geochim. Cosmochim. Acta* **67**, 4791–4806.

Flynn, G. J., H. Leroux, K. Tomenka, I. Ohnishi, T. Mikouchi, S. Wirick, L. P. Keller, C. Jacobsen, and S. A. Sandford 2008. Carbonate in comets: A comparison of comets 1P/Halley, 9P/Tempel 1, and 81P/Wild 2. Lunar Planet. Sci. Conf. 39, Abstract 1979.

Fries, M., M. J. Burchell, A. Kearsley, and S. A. 2009. Capture effects in carbonaceous material: A Stardust analogue study. *Meteoritics Planet. Sci.* **44**, 1465–1474.

Fulle, M., A. Levasseur-Regourd, N. McBride, and H. E. 2000. In-situ dust measurements from within the coma of 1P/Halley: First order approximation with a dust dynamical model. *A. J.* **119**, 1968–1977.

Furusho, R., Y. Ikeda, D. Kinoshita, W.-H. Ip, H. Kawakita, T. Kasuga, Y. Sato, H. C. Lin, M. S. Chang, Z. H. Lin, and J.-I. Watanabe 2007. Imaging polarimetry of comet 9P/Tempel 1 before and after the Deep Impact. *Icarus* **190**, 454–458.

Furusho, R., B. Suzuki, N. Yamamoto, H. Kawakita, T. Sasaki, Y. Shimizu, and T. Kurakami 1999. Imaging polarimetry and color of the inner coma of comet Hale-Bopp (C/1995 O1). *Pub. Ast. Soc. Japan* **51**, 367–473.

Gibb, E. L., B. P. Bonev, G. L. Villanueva, M. A. DiSanti, and M. J. Mumma 2013. Solar fluorescence model of CH_3D as applied to comet emission. *J. Mol. Spec.* **291**, 118–124.

Gicquel, A., D. Bockelée-Morvan, V. V. Zakharov, M. S. Kelley, C. E. Woodward, and D. H. Wooden 2012. Investigation of dust and water ice in comet

9P/Tempel 1 from Spitzer observations of the Deep Impact event. *Astr. and Ap.* **542**, A119.

Goesmann, F., H. Rosenbauer, R. Roll, C. Szopa, F. Raulin, R. Sternberg, G. Israel, U. Meierhenrich, W. Thiemann, and G. Munoz-Caro 2007. COSAC, the Cometary Sampling and Composition experiment on Philae. *Space Science Rev.* **128**, 257–280.

Green, S. F., J. K. Davies, T. R. Geballe, T. Brooke, and A. T. Tokunaga 1992. A strong 3.4 micron emission feature in comet Austin 1989c1. In *Asteroids, Comets, Meteors 1991* (A. W. Harris and E. Bowell, Eds.) pp. 211–214.

Greenberg, J. M. and J. I. Hage 1990. From interstellar dust to comets - a unification of observational constraints. *Ap. J.* **361**, 260–274.

Gulkis, S., M. Allen, P. von Allmen, G. Beaudin, N. Biver, D. Bockelée-Morvan, M. Choukroun, J. Crovisier, B. J. R. Davidsson, P. Encrenaz, T. Encrenaz, M. Frerking, P. Hartogh, M. Hofstadter, W.-H. Ip, M. Janssen, C. Jarchow, S. Keihm, S. Lee, E. Lellouch, C. Leyrat, L. Rezac, F. P. Schloerb, and T. Spilker 2015. Subsurface properties and early activity of comet 67P/Churyumov-Gerasimenko. *Science* **347**, 709.

Gulkis, S., M. Frerking, J. Crovisier, G. Beaudin, P. Hartogh, P. Encrenaz, T. Koch, C. Kahn, Y. Salinas, R. Nowicki, R. Irigoyen, M. Janssen, P. Stek, M. Hofstadter, M. Allen, C. Backus, L. Kamp, C. Jarchow, E. Steinmetz, A. Deschamps, J. Krieg, M. Gheudin, D. Bockelée-Morvan, N. Biver, T. Encrenaz, D. Despois, W. Ip, E. Lellouch, I. Mann, D. Muhleman, H. Rauer, P. Schloerb, and T. Spilker 2007. MIRO: Microwave Instrument for Rosetta Orbiter. *Space Science Rev.* **128**, 561–597.

Hadamcik, E. and A. C. Levasseur-Regourd 2003a. Dust coma of comet C/1999 S4 (LINEAR): Imaging polarimetry during nucleus disruption. *Icarus* **166**, 188–194.

Hadamcik, E. and A. C. Levasseur-Regourd 2003b. Imaging polarimetry of cometary dust: Different comets and phase angles. *J. Quant. Spectrosc. Radiat. Transfer* **79-80**, 661–678.

Hadamcik, E. and A. C. Levasseur-Regourd 2009. Optical properties of dust from Jupiter Family comets. *Plan. Space Sci.* **57**, 1118–1132.

Hadamcik, E., A. C. Levasseur-Regourd, V. Leroi, and D. Bardin 2007a. Imaging polarimetry of the dust coma of comet Tempel 1 before and after Deep Impact. *Icarus* **190**, 459–468.

Hadamcik, E., J.-B. Renard, A. Buch, N. Carrasco, N. Johnson, and J. Nuth 2014. Linear polarization of light scattered by cometary analogs: New samples. Asteroids, Comets, Meteors 2014 Helsinki, Finland.

Hadamcik, E., J.-B. Renard, F. J. M. Rietmeijer, A. C. Levasseur-Regourd, H. G. M. Hill, J. M. Karner, and J. A. Nuth 2007b. Light scattering by fluffy Mg-Fe-SiO and C mixtures as cometary analogs (PROGRA^2 experiment). *Icarus* **190**, 660–671.

Hadamcik, E., A. K. Sen, A. C. Levasseur-Regourd, R. Gupta, J. Lasue, and R. Botet 2013. Dust in comet 103P/Hartley 2 coma during EPOXI mission. *Icarus* **222**, 774–785.

Hanner, M. S. 1981. On the detectability of icy grains in the comae of comets. *Icarus* **47**, 342–350.

Hanner, M. S. 1999. The silicate material in comets. *Space Science Rev.* **90**, 99–108.

Hanner, M. S. and J. P. Bradley 2004. Composition and mineralogy of cometary dust. In *Comets II* (M. C. Festou, H. U. Keller, and H. A. Weaver, Eds.) pp. 555–564 Univ. of Arizona Press Tucson, AZ.

Harker, D. E., D. H. Wooden, C. E. Woodward, and C. Lisse 2002. Grain properties of comet C/1995 O1 (Hale-Bopp). *Ap. J.* **580**, 579–597.

Harker, D. E., D. H. Wooden, C. E. Woodward, and C. Lisse 2004. Erratum: Grain properties of comet C/1995 O1 (Hale-Bopp). *Ap. J.* **615**, 1081.

Harker, D. E., C. E. Woodward, and D. Wooden 2005. The dust grains from 9P/Tempel 1 before and after the encounter with Deep Impact. *Science* **310**, 278–280.

Harker, D. E., C. E. Woodward, D. H. Wooden, R. S. Fisher, and C. A. Trujillo 2007. Gemini-N mid-IR observations of the dust properties of the ejecta excavated from comet 9P/Tempel 1 during Deep Impact. *Icarus* **190**, 432–453.

Hässig, M., K. Altwegg, H. Balsiger, A. Bar-Nun, J. J. Berthelier, A. Bieler, P. Bochsler, C. Briois, U. Calmonte, M. Combi, J. De Keyser, P. Eberhardt, B. Fiethe, S. A. Fuselier, M. Galand, S. Gasc, T. I. Gombosi, K. C. Hansen, A. Jäckel, H. U. Keller, E. Kopp, A. Korth, E. Kührt, L. Le Roy, U. Mall, B. Marty, O. Mousis, E. Neefs, T. Owen, H. Rème, M. Rubin, T. Sémon, C. Tornow, C.-Y. Tzou, J. H. Waite, and P. Wurz 2015. Time variability and heterogeneity in the coma of 67P/Churyumov-Gerasimenko. *Science* **347**, 276.

Hayward, T. L., M. S. Hanner, and Z. Sekanina 2000. Thermal infrared imaging and spectroscopy of comet Hale-Bopp (C/1995 O1). *Ap. J.* **538**, 428–455.

Hines, D. C., G. Videen, . E. Zubko, K. Muinonen, Y. Shkuratov, V. G. Kaydash, M. Knight, M. L. Sitko, C. M. Lisse, M. Mutchler, D. Hammer, and P. A. Yanamandra-Fisher 2014. Hubble Space Telescope pre-perihelion

ACS/WFC Imaging Polarimetry of comet ISON (C/2012 S1) at 3.81 AU. *Ap. J.* **780**, L32–L38.

Hodapp, K. W., G. Aldering, K. J. Meech, A. L. Cochran, P. Antilogus, E. Pécontal, W. Chickering, N. Blanc, Y. Copin, D. K. Lynch, R. . Rudy, S. Mazuk, C. C. Venturini, R. C. Puetter, and R. B. Perry 2007. Visible and near-infrared spectrophotometry of the Deep Impact ejecta of comet 9P/Tempel 1. *Icarus* **187**, 185–198.

HÖrz, F., R. Bastien, J. Borg, J. P. Bradley, J. C. Bridges, D. E. Brownlee, M. J. Burchell, M. Chi, M. J. Cintala, Z. R. Dai, Z. Djouadi, G. Dominguez, T. E. Economou, S. A. J. Fairey, C. Floss, I. A. Franchi, G. A. Graham, S. F. Green, P. Heck, P. Hoppe, J. Huth, H. Ishii, A. T. Kearsley, J. Kissel, J. Leitner, H. Leroux, K. Marhas, K. Messenger, C. S. Schwandt, T. H. See, C. Snead, F. J. Stadermann, T. Stephan, R. Stroud, N. Teslich, J. M. Trigo-Rodríguez, A. J. Tuzzolino, D. Troadec, P. Tsou, J. Warren, A. Westphal, P. Wozniakiewicz, I. Wright, and E. Zinner 2006. Impact features on Stardust: Implications for comet 81P/Wild 2 dust. *Science* **314**, 1716.

Jehin, E., J. Manfroid, H. Kawakita, D. Hutsemékers, M. Weiler, C. Arpigny, A. Cochran, O. Hainaut, H. Rauer, R. Schulz, and J.-M. Zucconi 2008. Optical spectroscopy of the B and C fragments of comet 73P/Schwassmann-Wachmann 3 at the ESO VLT. LPI Contributions **1405**, p.8319.

Jessberger, E. 1999. Rocky cometary particulates: Their elemental, isotopic, and mineralogical ingredients. *Space Science Rev.* **90**, 91–97.

Jewitt, D. and K. J. Meech 1986. Cometary grain scattering versus wavelength, or, "What color is comet dust?". *Ap. J.* **310**, 937–952.

Jones, T. J. and R. D. Gehrz 2000. Infrared imaging polarimetry of comet C/1995 O1 (Hale-Bopp). *Icarus* **143**, 338–346.

Joswiak, D. J., D. E. Brownlee, G. Matrajt, A. J. Westphal, C. J. Snead, and Z. Gainsforth 2012. Comprehensive examination of large mineral and rock fragments in Stardust tracks: Mineralogy, analogous extraterrestrial materials, and source regions. *Meteoritics Planet. Sci.* **47**, 471–524.

Kawakita, H., N. Dello Russo, R. Vervack, Jr., H. Kobayashi, M. A. DiSanti, C. Opitom, E. Jehin, H. A. Weaver, A. L. Cochran, W. M. Harris, D. Bockelée-Morvan, N. Biver, J. Crovisier, A. J. McKay, J. Manfroid, and M. Gillon 2014. Extremely organic-rich coma of comet C/2010 G2 (Hill) during its outburst in 2012. *Ap. J.* **788**, 110.

Kawakita, H., H. Kobayashi, N. Dello Russo, R. J. Vervack, M. Hashimoto, H. A. Weaver, C. M. Lisse, A. L. Cochran, W. M. Harris, D. Bockelée-Morvan, N. Biver, J. Crovisier, and A. J. McKay 2013. Parent volatiles in comet 103P/Hartley 2 observed by Keck II with NIRSPEC during the 2010 apparition. *Icarus* **222**, 723–733.

Kawakita, H. and M. J. Mumma 211. Fluorescence excitation models of ammonia and amidogen radical (NH_2) in comets: Application to comet C/2004 Q2 (Machholz). *Ap. J.* **727**, 91.

Kawakita, H., J.-i. Watanabe, T. Ootsubo, R. Nakamura, T. Fuse, N. Takato, S. Sasaki, and T. Sasaki 2004. Evidence of icy grains in comet C/2002 T7 (LINEAR) at 3.52 AU. *Ap. J.(Letters)* **601**, L191–L194.

Keller, H. U., C. Arpigny, C. Barbieri, R. M. Bonnet, S. Cazes, M. Coradini, C. B. Cosmovici, W. A. Delamere, W. F. Huebner, D. W. Hughes, C. Jamar, D. Malaise, H. J. Reitsema, H. U. Schmidt, W. K. H. Schmidt, P. Seige, F. L. Whipple, and K. Wilhelm 1986. First Halley multicolour camera imaging results from Giotto. *Nature* **321**, 320–326.

Keller, L. P., S. Bajt, G. A. Baratta, J. Borg, J. P. Bradley, D. E. Brownlee, H. Busemann, J. R. Brucato, M. Burchell, L. Colangeli, L. D'Hendecourt, Z. Djouadi, G. Ferrini, G. Flynn, I. A. Franchi, M. Fries, M. M. Grady, G. A. Graham, F. Grossemy, A. Kearsley, G. Matrajt, K. Nakamura-Messenger, V. Mennella, L. Nittler, M. E. Palumbo, F. J. Stadermann, P. Tsou, A. Rotundi, S. A. Sandford, C. Snead, A. Steele, D. Wooden, and M. Zolensky 2006. Infrared spectroscopy of comet 81P/Wild 2 samples returned by Stardust. *Science* **314**, 1728–.

Kelley, M. S., D. J. Lindler, D. Bodewits, M. F. A'Hearn, C. M. Lisse, L. Kolokolova, J. Kissel, and B. Hermalyn 2013. A distribution of large particles in the coma of comet 103P/Hartley 2. *Icarus* **222**, 634–652.

Kelley, M. S. and D. H. Wooden 2009. The composition of dust in Jupiter-family comets inferred from infrared spectroscopy. *Plan. and Space Sci.* **57**, 1133–1145.

Kiselev, N. N., K. Jockers, and T. Bonev 2004. CCD imaging polarimetry of comet 2P/Encke. *Icarus* **168**, 385–391.

Kiselev, N. N., K. Jockers, V. K. Rosenbush, and P. P. Korsun 2001. Analysis of polarimetric, photometric, and spectroscopic observations of comet C/1996 Q1 (Tabur). *Sol. Syst. Res.* **35**, 480–495.

Kiselev, N. N., K. Jockers, V. K. Rosenbush, F. P. Velichko, T. Bonev, and N. Karpov 2000. Anomalous wavelength dependence of polarization of comet 21P/Giacobini-Zinner. *Plan. and Space Sci.* **48**, 1005–1009.

Kiselev, N. N., V. Rosenbush, A. C. Levasseur-Regourd, and L. Kolokolova 2014. Polarimetry of comets. In *Polarization of stars and planetary systems* (L. Kolokolova, J. Hough, and A. C. Levasseur-Regourd, Eds.) pp. 379–404 Cambridge University Press Cambridge, UK.

Kissel, J., K. Altwegg, B. C. Clark, L. Colangeli, H. Cottin, S. Czempiel, J. Eibl, C. Engrand, H. M. Fehringer, B. Feuerbacher, M. Fomenkova, A. Glasmachers, J. M. Greenberg, E. Grün, G. Haerendel, H. Henkel, M. Hilchenbach, H. von Hoerner, H. Höfner, K. Hornung, E. K. Jessberger, A. Koch, H. Krüger, Y. Langevin, P. Parigger, F. Raulin, F. Rüdenauer, J. Rynö, E. R. Schmid, R. Schulz, J. Silén, W. Steiger, T. Stephan, L. Thirkell, R. Thomas, K. Torkar, N. G. Utterback, K. Varmuza, K. P. Wanczek, W. Werther, and H. Zscheeg 2007. COSIMA high resolution time-of-flight secondary ion mass spectrometer for the analysis of cometary dust particles onboard Rosetta. *Space Science Rev.* **128**, 823–867.

Kissel, J., D. E. Brownlee, K. Buchler, B. C. Clark, H. Fechtig, E. Grün, K. Hormung, E. B. Igenbergs, E. K. Jessberger, F. R. Krueger, H. Kuczera, J. A. M. McDonnell, G. M. Morfill, J. Rahe, G. H. Schwehm, Z. Sekanina, N. G. Utterback, H. J. Volk, and H. A. Zook 1986. Composition of comet Halley dust particles from Giotto observations. *Nature* **321**, 336–337.

Kissel, J., F. R. Krueger, J. Silén, and B. C. Clark 2004. The cometary and interstellar dust analyzer at comet 81P/Wild 2. *Science* **304**, 1774–1776.

Kissel, J., R. Z. Sagdeev, J. L. Bertaux, V. N. Angarov, J. Audouze, J. E. Blamont, K. Buckler, E. N. Evlanov, H. Fechtig, M. N. Fomenkova, H. von Hoerner, N. A. Inogamov, V. N. Khromov, W. Knabe, F. R. Krueger, Y. Langevin, V. B. Leonas, L.-R. A. C., G. G. Managadz, S. N. Podkolzin, V. D. Shapiro, S. R. Tabaldyev, and B. V. Zubkov 1986. Composition of comet Halley dust particles from Vega observations. *Nature* **321**, 280–282.

Kleine, M., S. Wyckoff, P. A. Wehinger, and B. A. Peterson 1995. The carbon isotope abundance ratio in comet Halley. *Ap. J.* **439**, 1021–1033.

Klingelhöfer, G., J. Brückner, C. D'Uston, R. Gellert, and R. Rieder 2007. The Rosetta Alpha Particle X-ray Spectrometer (APXS). *Space Science Rev.* **128**, 383–396.

Knight, M. M., K. J. Walsh, M. F. A'Hearn, R. A. Swaters, B. A. Zauderer, N. H. Samarasinha, R. Vázquez, and H. Reitsema 2007. Ground-based visible and near-IR observations of comet 9P/Tempel 1 during the Deep Impact encounter. *Icarus* **187**, 199–207.

Kobayashi, H., H. Kawakita, M. J. Mumma, B. P. Bonev, J.-i. Watanabe, and T. Fuse 2007. Organic volatiles in comet 73P-B/Schwassmann-Wachmann 3

observed during its outburst: A clue to the formation region of the Jupiter-Family comets. *Ap. J.(Letters)* **668**, L75–L78.

Kofman, W., A. Herique, J.-P. Goutail, T. Hagfors, I. P. Williams, E. Nielsen, J.-P. Barriot, Y. Barbin, C. Elachi, P. Edenhofer, A.-C. Levasseur-Regourd, D. Plettemeier, G. Picardi, R. Seu, and V. Svedhem 2007. The COmet Nucleus Sounding Experiment by Radiowave Transmission (CONSERT): A short description of the instrument and of the commissioning stages. *Space Science Rev.* **128**, 413–432.

Kolokolova, L., M. S. Hanner, A. C. Levasseur-Regourd, and B. A. S. Gustavson 2004. Physical properties of cometary dust from light scattering and thermal emission. In *Comets II* (M. C. Festou, H. U. Keller, and H. A. Weaver, Eds.) pp. 577–604 Univ. of Arizona Press Tucson, AZ.

Kolokolova, L., J. Hough, and A. C. Levasseur-Regourd 2015. *Polarization of Stars and Planetary Systems*. Cambridge University Press, Cambridge, UK.

Kolokolova, L., H. Kimura, N. Kiselev, and V. Rosenbush 2007. Two different evolutionary types of comets proved by polarimetry and infrared properties of their dust. *Astr. and Ap.* **463**, 1189–1196.

Krueger, F. R., A. Korth, and J. Kissel 1991. The organic matter of comet Halley as inferred by joint gas phase and solid phase analyses. *Space Science Rev.* **56**, 167–175.

Langland-Shula, L. E. and G. H. Smith 2011. Comet classification with new methods for gas and dust spectroscopy. *Icarus* **213**, 280–322.

Lasue, J., A. C. Levasseur-Regourd, E. Hadamcik, and G. Alcouffe 2009. Cometary dust properties retrieved from polarization observations: Application to C/1995 O1 Hale-Bopp and 1P/Halley. *Icarus* **199**, 129–144.

Le Roy, L., G. Briani, C. Briois, H. Cottin, N. Fray, L. Thirkell, G. Poulet, and M. Hilchenbach 2012. On the prospective detection of polyoxymethylene in comet 67P/Churyumov-Gerasimenko with the COSIMA instrument onboard Rosetta. *Plan. Space Sci.* **65**, 83–92.

Lellouch, E., J. Crovisier, T. Lim, D. Bockelée-Morvan, K. Leech, M. S. Hanner, B. Altieri, B. Schmitt, F. Trotta, and H. U. Keller 1998. Evidence for water ice and estimate of dust production rate in comet Hale-Bopp at 2.9 AU from the Sun. *Astr. and Ap.* **339**, L9–L12.

Levasseur-Regourd, A. C., E. Hadamcik, and J. B. Renard 1996. Evidence of two classes of comets from their polarimetric properties at large phase angles. *Astr. and Ap.* **313**, 327–333.

Levasseur-Regourd, A. C., N. McBride, E. Hadamcik, and M. Fulle 1999. Similarities between in situ measurements of local dust scattering and dust flux impact data within the coma of 1P/Halley. *Astr. and Ap.* **348**, 636–641.

Levasseur-Regourd, A. C., M. Zolensky, and J. Lasue 2008. Dust in cometary comae: Present understanding of the structure and composition of dust particles. *Planet. Space Sci.* **56**, 1719–1724.

Lim, Y.-M., K.-W. Min, P. D. Feldman, W. Han, and J. Edelstein 2014. Far-ultraviolet observations of comet C/2001 Q4 (NEAT) with FIMS/SPEAR. *Ap. J.* **781**, 80.

Lippi, M., G. L. Villanueva, M. A. DiSanti, H. Böhnhardt, M. J. Mumma, B. P. Bonev, and D. Prialnik 2013. A new model for the ν_1 vibrational band of HCN in cometary comae, with application to three comets. *Astr. and Ap.* **551**, A51.

Lisse, C. M., K. E. Kraemer, J. A. Nuth, A. Li, and D. Joswiak 2007. Comparison of the composition of the Tempel 1 ejecta to the dust in comet C/Hale Bopp 1995 O1 and YSO HD 100546. *Icarus* **187**, 69–86.

Liu, X., D. E. Shemansky, J. T. Hallett, and H. A. Weaver 2007. Extreme non-LTE H_2 in comets C/2000 WM1 (LINEAR) and C/2001 A2 (LINEAR). *Ap. J. Suppl.* **169**, 458–471.

Lupu, R. E., P. D. Feldman, H. A. Weaver, and G.-P. Tozzi 2007. The fourth positive system of carbon monoxide in the Hubble Space Telescope spectra of comets. *Ap. J.* **670**, 1473–1484.

Manfroid, J., E. Jehin, D. Hutsemékers, A. Cochran, J.-M. Zucconi, C. Arpigny, R. Schulz, J. Stüwe, and I. Liyin 2009. The CN isotopic ratios in comets. *Astr. and Ap.* **503**, 613–624.

Manfroid, J., E. Jehin, D. Hutsemékers, A. Cochran, J.-M. Zucconi, C. Arpigny, R. Schulz, and J. A. Stüwe 2005. Isotopic abundance of nitrogen and carbon in distant comets. *Astr. and Ap.* **432**, L5–L8.

Matrajt, G., M. Ito, S. Wirick, S. Messenger, D. E. Brownlee, D. Joswiak, G. Flynn, S. Sandford, C. Snead, and A. Westphal 2008. Carbon investigation of two Stardust particles: A TEM, NanoSIMS, and XANES study. *Meteoritics Planet. Sci.* **43**, 315–334.

Matzel, J. E. P., H. A. Ishii, D. Joswiak, I. D. Hutcheon, J. P. Bradley, D. Brownlee, P. K. Weber, N. Teslich, G. Matrajt, K. D. McKeegan, and G. J. MacPherson 2010. Constraints on the formation age of cometary material from the NASA Stardust Mission. *Science* **328**, 483–.

McKay, A., A. Cochran, N. Dello Russo, H. Weaver, R. Vervack, W. Harris, H. Kawakita, M. DiSanti, N. Chanover, and Z. Tsvetanov 2014. Evolution of fragment-species production in comet C/2012 S1 (ISON) from 1.6 au to 0.4 au. Asteroids, Comets, Meteors 2014, Helsinki, Finland.

McKay, A. J., N. J. Chanoveer, J. P. Morgenthaler, A. L. Cochran, W. M. Harris, and N. Dello Russo 2013. Observations of the forbidden oxygen lines in DIXI target comet 103P/Hartley. *Icarus* **222**, 684–690.

McKay, A. J., N. J. Chanover, J. P. Morgenthaler, A. L. Cochran, W. M. Harris, and N. D. Russo 2012. Forbidden oxygen lines in comets C/2006 W3 Christensen and C/2007 Q3 Siding Spring at large heliocentric distance: Implications for the sublimation of volatile ices. *Icarus* **220**, 277–285.

McKeegan, K. D., J. Aléon, J. Bradley, D. Brownlee, H. Busemann, A. Butterworth, M. Chaussidon, S. Fallon, C. Floss, J. Gilmour, M. Gounelle, G. Graham, Y. Guan, P. R. Heck, P. Hoppe, I. D. Hutcheon, J. Huth, H. Ishii, M. Ito, S. Jacobsen, A. Kearsley, L. A. Leshin, M.-C. Liu, A. Lyon, K. Marhas, B. Marty, G. Matrajt, A. Meibom, S. Messenger, S. Mostefaoui, S. Mukhopadhyay, K. Nakamura-Messenger, L. Nittler, R. Palma, R. O. Pepin, D. A. Papanastassiou, F. Robert, D. Schlutter, C. J. Snead, F. Stadermann, R. Stroud, P. Tsou, A. Westphal, E. D. Young, K. Ziegler, L. Zimmermann, and E. Zinner 2006. Isotopic compositions of cometary matter returned by Stardust. *Science* **314**, 1724–.

Meier, R. and M. F. A'Hearn 1997. Atomic sulfur in cometary comae based on UV spectra of the S I triplet near 1814 å. *Icarus* **125**, 164–194.

Moreels, G., J. Clairemidi, P. Hermine, P. Brechignac, and P. Rousselot 1994. Detection of a polycyclic aromatic molecule in comet P/Halley. *Astr. and Ap.* **282**, 643–656.

Morgenthaler, J. P., W. M. Harris, M. R. Combi, P. D. Feldman, and H. A. Weaver 2009. The GALEX comets. AAS/Division for Planetary Sciences Meeting Abstracts.

Morgenthaler, J. P., W. M. Harris, M. R. Combi, P. D. Feldman, and H. A. Weaver 2011. GALEX FUV observations of comet C/2004 Q2 (Machholz): The ionization lifetime of carbon. *Ap. J.* **726**, 8.

Mumma, M. J. and S. B. Charnley 2011. The chemical composition of comets – Emerging taxonomies and natal heritage. *Ann. Rev. Astr. Ap.* **49**, 471–524.

Mumma, M. J., M. A. DiSanti, K. Magee-Sauer, B. P. Bonev, G. L. Villanueva, H. Kawakita, N. Dello Russo, E. L. Gibb, G. A. Blake, J. E.

Lyke, R. D. Campbell, J. Aycock, A. Conrad, and G. M. Hill 2005. Parent volatiles in comet 9P/Tempel 1: Before and after impact. *Science* **310**, 270–274.

Mumma, M. J., I. S. McLean, M. A. DiSanti, J. E. Larkin, N. Dello Russo, K. Magee-Sauer, E. E. Becklin, T. Bida, F. Chafee, A. R. Conrad, D. F. Figer, A. M. Gilbert, J. R. Graham, N. A. Levenson, R. E. Novak, D. C. Reuter, H. I. Teplitz, M. K. Wilcox, and L.-H. Xu 2001. A survey of organic volatile species in comet C/1999 H1 (Lee) using NIRSPEC at the Keck Observatory. *Ap. J.* **546**, 1183–1193.

Mumma, M. J., H. A. Weaver, and H. P. Larson 1987. The ortho-para ratio of water vapor in comet P/Halley. *Astr. and Ap.* **187**, 419–424.

Nakashima, D., T. Ushikubo, D. J. Joswiak, D. E. Brownlee, G. Matrajt, M. K. Weisberg, M. E. Zolensky, and N. T. Kita 2012. Oxygen isotopes in crystalline silicates of comet Wild 2: A comparison of oxygen isotope systematics between Wild 2 particles and chondritic materials. *Earth Plan. Sci. Let.* **357**, 355–365.

Newburn, R. L. and H. Spinrad 1984. Spectrophotometry of 17 comets. I. The emission features. *A. J.* **89**, 289–309.

Newburn, R. L. and H. Spinrad 1989. Spectrophotometry of 25 comets: Post-Halley updates for 17 comets plus new observations for eight additional comets. *A. J.* **97**, 552–569.

Ogliore, R. C., G. R. Huss, K. Nagashima, A. L. Butterworth, Z. Gainsforth, J. Stodolna, A. J. Westphal, D. Joswiak, and T. Tyliszczak 2012. Incorporation of a late-forming chondrule into comet Wild 2. *Ap. J.* **745**, L19.

Ootsubo, T., H. Kawakita, S. Hamada, H. Kobayashi, M. Yamaguchi, F. Usui, T. Nakagaw, M. Ueno, M. Ishiguro, T. Sekiguchi, J. Watanabe, I. Sakon, T. Shimonishi, and T. Onaka 2012. AKARI near-infrared spectroscopic survey for CO_2 in 18 comets. *Ap. J.* **752**, 15.

Opitom, C., E. Jehin, J. Manfroid, D. Hutsemakers, and M. Gillon 2014. TRAPPIST monitoring of C/2012 S1 (ISON) and C/2013 R1 (Lovejoy). Asteroids, Comets, Meteors 2014, Helsinki, Finland.

Paganini, L., M. A. DiSanti, M. J. Mumma, G. L. Villanueva, B. P. Bonev, J. V. Keane, E. L. Gibb, H. Boehnhardt, and K. J. Meech 2014. The unexpectedly bright comet C/2012 F6 (Lemmon) unveiled at near-infrared wavelengths. *A. J.* **147**, 15.

Paganini, L., M. J. Mumma, G. L. Villanueva, M. A. DiSanti, and B. P. Bonev 2015. The volatile composition of comet C/2003 K4 (LINEAR) at near-IR

wavelengths Comparisons with results from the Nancay radio observatory and from the Odin, Spitzer, and SOHO space telescopes. Ap. J. (in press, 2015).

Paganini, L., M. J. Mumma, G. L. Villanueva, J. V. Keane, G. A. Blake, B. P. Bonev, M. A. DiSanti, E. L. Gibb, and K. J. Meech 2014. C/2013 R1 (Lovejoy) at IR wavelengths and the variability of CO abundances among Oort Cloud comets. *Ap. J.* **791**, 122.

Preston, G. W. 1967. The spectrum of comet Ikeya-Seki (1965f). *Ap. J.* **147**, 718–742.

Protopapa, S., J. M. Sunshine, L. M. Feaga, M. S. P. Kelley, M. F. A'Hearn, T. L. Farnham, O. Groussin, S. Besse, F. Merlin, and J.-Y. Li 2014. Water ice and dust in the innermost coma of comet 103P/Hartley 2. *Icarus* **238**, 191–204.

Radeva, Y. L., M. J. Mumma, G. L. Villanueva, and M. F. A'Hearn 2011. A newly developed fluorescence model for C_2H_6 ν_5 and application to cometary spectra acquired with NIRSPEC at Keck II. *Ap. J.* **729**, 135.

Radeva, Y. L., M. J. Mumma, G. L. Villanueva, B. P. Bonev, M. A. DiSanti, M. F. A'Hearn, and N. Dello Russo 2013. High-resolution infrared spectroscopic measurements of comet 2P/Encke: Unusual organic composition and low rotational temperatures. *Icarus* **223**, 298–307.

Reach, W. T., M. S. Kelley, and J. Vaubaillon 2013. Survey of cometary CO_2, CO, and particulate emissions using the Spitzer Space Telescope. *Icarus* **226**, 777–797.

Renard, J. B., A. C. Levasseur-Regourd, and A. Dolfus 1992. Polarimetric CCD imaging of comet Levy. *Ann. Geophys.* **10**, 288–292.

Riedler, W., K. Torkar, H. Jeszenszky, J. Romstedt, H. S. C. Alleyne, H. Arends, W. Barth, J. V. D. Biezen, B. Butler, P. Ehrenfreund, M. Fehringer, G. Fremuth, J. Gavira, O. Havnes, E. K. Jessberger, R. Kassing, W. Klöck, C. Koeberl, A. C. Levasseur-Regourd, M. Maurette, F. Rüdenauer, R. Schmidt, G. Stangl, M. Steller, and I. Weber 2007. MIDAS - the Micro-Imaging Dust Analysis System for the Rosetta Mission. *Space Science Rev.* **128**, 869–904.

Rubin, M., K. Altwegg, H. Balsiger, A. Bar-Nun, J.-J. Berthelier, A. Bieler, P. Bochsler, C. Briois, U. Calmonte, M. Combi, J. De Keyser, F. Dhooghe, P. Eberhardt, B. Fiethe, S. A. Fuselier, S. Gasc, T. I. Gombosi, K. C. Hansen, M. Hässig, A. Jäckel, E. Kopp, A. Korth, L. Le Roy, U. Mall, B. Marty, O. Mousis, T. Owen, H. Rème, T. Sémon, C.-Y. Tzou, J. H. Waite, and P. Wurz 2015. Molecular nitrogen in comet 67P/Churyumov-Gerasimenko indicates a low formation temperature. *Science* **348**, 232–235.

Sandford, S. A., J. Aléon, C. M. O. Alexander, T. Araki, S. Bajt, G. A. Baratta, J. Borg, J. P. Bradley, D. E. Brownlee, J. R. Brucato, M. J. Burchell, H. Busemann, A. Butterworth, S. J. Clemett, G. Cody, L. Colangeli, G. Cooper, L. D'Hendecourt, Z. Djouadi, J. P. Dworkin, G. Ferrini, H. Fleckenstein, G. J. Flynn, I. A. Franchi, M. Fries, M. K. Gilles, D. P. Glavin, M. Gounelle, F. Grossemy, C. Jacobsen, L. P. Keller, A. L. D. Kilcoyne, J. Leitner, G. Matrajt, A. Meibom, V. Mennella, S. Mostefaoui, L. R. Nittler, M. E. Palumbo, D. A. Papanastassiou, F. Robert, A. Rotundi, C. J. Snead, M. K. Spencer, F. J. Stadermann, A. Steele, T. Stephan, P. Tsou, T. Tyliszczak, A. J. Westphal, S. Wirick, B. Wopenka, H. Yabuta, R. N. Zare, and M. E. Zolensky 2006. Organics captured from comet 81P/Wild 2 by the Stardust spacecraft. *Science* **314**, 1720–.

Schleicher, D. G. 2008. The extremely anomalous molecular abundances of comet 96P/Machholz 1 from narrowband photometry. *A. J.* **136**, 2204–2213.

Schleicher, D. G. and A. N. Bair 2011. The composition of the interior of comet 73P/Schwassmann-Wachmann 3: Results from narrowband photometry of multiple components. *A. J.* **141**, 177–.

Schleicher, D. G. and A. N. Bair 2014. Compositional taxonomy for comets: Background and motivation. Asteroids, Comets, Meteors 2014, Helsinki, Finland.

Schleicher, D. G., K. L. Barnes, and N. F. Baugh 2006. Photometry and imaging reults for comet 9P/Tempel 1 and Deep Impact: Gas production rates, postimpact light curves, and ejecta plume morphology. *A. J.* **131**, 1130–1137.

Schleicher, D. G. and T. L. Farnham 2004. Photometry and imaging of the coma with narrowband filters. In *Comets II* (M. C. Festou, H. U. Keller, and H. A. Weaver, Eds.) pp. 449–469 Univ. of Arizona Press Tucson, AZ.

Schultz, P. H., B. Hermalyn, and J. Veverka 2013. The Deep Impact crater on 9P/Tempel 1 from Stardust-NExT. *Icarus* **222**, 502–515.

Schulz, R., M. Hilchenbach, Y. Langevin, J. Kissel, J. Silen, C. Briois, C. Engrand, K. Hornung, D. Baklouti, A. Bardyn, H. Cottin, H. Fischer, N. Fray, M. Godard, H. Lehto, L. Le Roy, S. Merouane, F.-R. Orthous-Daunay, J. Paquette, J. Rynö, S. Siljeström, O. Stenzel, L. Thirkell, K. Varmuza, and B. Zaprudin 2015. Comet 67P/Churyumov-Gerasimenko sheds dust coat accumulated over the past four years. *Nature* **518**, 216–218.

Schulz, R., A. Owens, P. M. Rodriguez-Pascual, D. Lumb, C. Erd, and J. A. Stüwe 2006. Detection of water ice grains after the Deep Impact onto comet 9P/Tempel 1. *Astr. and Ap.* **448**, L53–L56.

Shinnaka, Y., H. Kawakita, H. Kobayashi, E. Jehin, J. Manfroid, D. Hutsemékers, and C. Arpigny 2011. Ortho-to-para abundance ratio (OPR) of ammonia in 15 comets: OPRs of ammonia versus $^{14}N/^{15}N$ ratios in CN. *Ap. J.* **729**, 81.

Sitko, M. L., D. K. Lynch, R. W. Russell, and M. S. Hanner 2004. 3–14 micron spectroscopy of comets C/2002 Q4 (Hoenig), C/2002 V1 (NEAT), C/2002 X5 (Kudo-Fukikawa), C/2002 Y1 (Juels-Holvorcem), and 69P/Taylor and the relationships among grain temperature, silicate band strength, and structure among comet families. *Ap. J.* **612**, 576–587.

Slaughter, C. D. 1969. The emission spectrum of comet Ikeya-Seki 1965-f at perihelion passage. *A. J.* **74**, 929–943.

Spencer, M. K. and R. N. Zare 2007. Comment on "Organics captured from comet 81P/Wild 2 by the Stardust spacecraft". *Science* **317**, 1680.

Stern, S. A., D. C. Slater, J. Scherrer, J. Stone, M. Versteeg, M. F. A'Hearn, J. L. Bertaux, P. D. Feldman, M. C. Festou, J. W. Parker, and O. H. W. Siegmund 2007. Alice: The Rosetta Ultraviolet imaging spectrograph. *Space Science Rev.* **128**, 507–527.

Sugita, S., T. Kadono, S. Sako, T. Ootsubo, M. Honda, H. Kawakita, R. Furusho, and J. Watanabe 2007. Mid-IR observations of Deep Impact reveal the primordial origin of a surface of comet 9P/Tempe1 1. In *Lunar and Planetary Science Conference* p. 1911.

Sunshine, J. M., O. Groussin, P. H. Schultz, M. F. A'Hearn, L. M. Feaga, T. L. Farnham, and K. P. Klaasen 2007. The distribution of water ice in the interior of comet Tempel 1. *Icarus* **190**, 284–294.

Thackeray, A. D., M. W. Feast, and B. Warner 1966. Daytime spectra of comet Ikeya-Seki near perihelion. *Ap. J.* **143**, 276–279.

Tuzzolino, A. J., T. E. Economou, B. C. Clark, P. Tsou, D. E. Brownlee, S. F. Green, J. A. M. McDonnell, N. McBride, and M. T. S. H. Colwell 2004. Dust measurements in the coma of Comet 81P/Wild 2 by the dust flux monitor instrument. *Science* **304**, 1776–1780.

Villanueva, G. L., M. A. DiSanti, M. J. Mumma, and L.-H. Xu 2012a. A quantum band model of the ν_3 fundamental of methanol (CH_3OH) and its application to fluorescence spectra of comets. *Ap. J.* **747**, 37.

Villanueva, G. L., M. J. Mumma, B. P. Bonev, R. E. Novak, R. J. Barber, and M. A. DiSanti 2012b. Water in planetary and cometary atmospheres: H_2O and HDO transmittance and fluorescence models. *J. Quant. Spectrosc. Radiat. Transfer* **113**, 202–220.

Villanueva, G. L., M. J. Mumma, R. E. Novak, Y. L. Radeva, H. U. Käufl, A. Smette, A. Tokunaga, A. Khayat, T. Encrenaz, and P. Hartogh 2013. A sensitive search for organics (CH_4, CH_3OH, H_2CO, C_2H_6, C_2H_2, C_2H_4), hydroperoxyl (HO_2), nitrogen compounds (N_2O, NH_3, HCN) and chlorine species (HCl, CH_3Cl) on Mars using ground-based high-resolution infrared spectroscopy. *Icarus* **223**, 11–27.

Weaver, H. A., P. D. Feldman, M. F. A'Hearn, N. Dello Russo, and S. A. Stern 2011. The carbon monoxide abundance in comet 103P/Hartley 2 during the EPOXI flyby. *Ap. J.(Letters)* **734**, L5.

Whipple, F. L. 1950. A comet model: The acceleration of comet Encke. *Ap. J.* **111**, 375–394.

Wooden, D. H. 2002. Comet grains: Their IR emission and their relation to ISM grains. *Earth, Moon, Planets* **89**, 247–287.

Wooden, D. H., C. E. Woodward, and D. E. Harker 2004. Discovery of crystalline silicates in comet C/2001 Q4 (NEAT). *Ap. J.* **612**, L77–L80.

Woodward, C. E., T. J. Jones, B. Brown, E. L. Ryan, M. Krejny, L. Kolokolova, M. S. Kelley, D. E. Harker, and M. L. Sitko 2011. Dust in comet C/2007 N3 (Lulin). *A. J.* **141**, 181–190.

Wright, I. P., S. J. Barber, G. H. Morgan, A. D. Morse, S. Sheridan, D. J. Andrews, J. Maynard, D. Yau, S. T. Evans, M. R. Leese, J. C. Zarnecki, B. J. Kent, N. R. Waltham, M. S. Whalley, S. Heys, D. L. Drummond, R. L. Edeson, E. C. Sawyer, R. F. Turner, and C. T. Pillinger 2007. Ptolemy-an instrument to measure stable isotopic ratios of key volatiles on a cometary nucleus. *Space Science Rev.* **128**, 363–381.

Yang, B., D. Jewitt, and S. Bus 2009. Comet 17P/Holmes in outburst: The near-infrared spectrum. *A. J.* **137**, 4538–4546.

Yang, B., J. Keane, K. Keech, T. Owen, and R. Wainscoat 2014. Multi-wavelength observations of comet C/20122 L4 (Pan-STARRS). *Ap. J.* **784**, L23–L27.

Zolensky, M., D. Frank, and L. Le 2011. Olivine and pyroxene compositions in fine-grained chondritic materials. Lunar Planet. Sci. Conf. 42, Abstract 1898.

Zolensky, M., K. Nakamura-Messenger, F. Rietmeijer, H. Leroux, T. Mikouchi, K. Ohsumi, S. Simon, L. Grossman, T. Stephan, M. Weisberg, M. Velbel, T. Zega, R. Stroud, K. Tomeoka, I. Ohnishi, N. Tomioka, T. Nakamura, G. Matrajt, D. Joswiak, D. Brownlee, F. Langenhorst, A. Krot, A. Kearsley, H. Ishii, G. Graham, Z. R. Dai, M. Chi, J. Bradley, K. Hagiya, M. Gounelle, and J. Bridges 2008. Comparing Wild 2 particles to chondrites and IDPs. *Meteoritics Planet. Sci.* **43**, 261–272.

Zolensky, M. E., T. J. Zega, H. Yano, S. Wirick, A. J. Westphal, M. K. Weisberg, I. Weber, J. L. Warren, M. A. Velbel, A. Tsuchiyama, P. Tsou, A. Toppani, N. Tomioka, K. Tomeoka, N. Teslich, M. Taheri, J. Susini, R. Stroud, T. Stephan, F. J. Stadermann, C. J. Snead, S. B. Simon, A. Simionovici, T. H. See, F. Robert, F. J. M. Rietmeijer, W. Rao, M. C. Perronnet, D. A. Papanastassiou, K. Okudaira, K. Ohsumi, I. Ohnishi, K. Nakamura-Messenger, T. Nakamura, S. Mostefaoui, T. Mikouchi, A. Meibom, G. Matrajt, M. A. Marcus, H. Leroux, L. Lemelle, L. Le, A. Lanzirotti, F. Langenhorst, A. N. Krot, L. P. Keller, A. T. Kearsley, D. Joswiak, D. Jacob, H. Ishii, R. Harvey, K. Hagiya, L. Grossman, J. N. Grossman, G. A. Graham, M. Gounelle, P. Gillet, M. J. Genge, G. Flynn, T. Ferroir, S. Fallon, D. S. Ebel, Z. R. Dai, P. Cordier, B. Clark, M. Chi, A. L. Butterworth, D. E. Brownlee, J. C. Bridges, S. Brennan, A. Brearley, J. P. Bradley, P. Bleuet, P. A. Bland, and R. Bastien 2006. Mineralogy and petrology of comet 81P/Wild 2 nucleus samples. *Science* **314**, 1735.

Zubko, E., R. Furusho, K. Kawabata, T. Yamamoto, K. Muinonen, and G. Videen 2011. Interpretation of photopolarimetric observations of comet 17P/Holmes. *J. Quant. Spectrosc. Radiat. Transfer* **112**, 1848–1863.

Zubko, E., K. Muinonen, Y. Shkuratov, E. Hadamcik, and A. C. Levasseur-Regourd 2012. Evaluating the carbon depletion found by the Stardust mission in comet 81P/Wild 2. *Astr. and Ap.* **544**, L8.

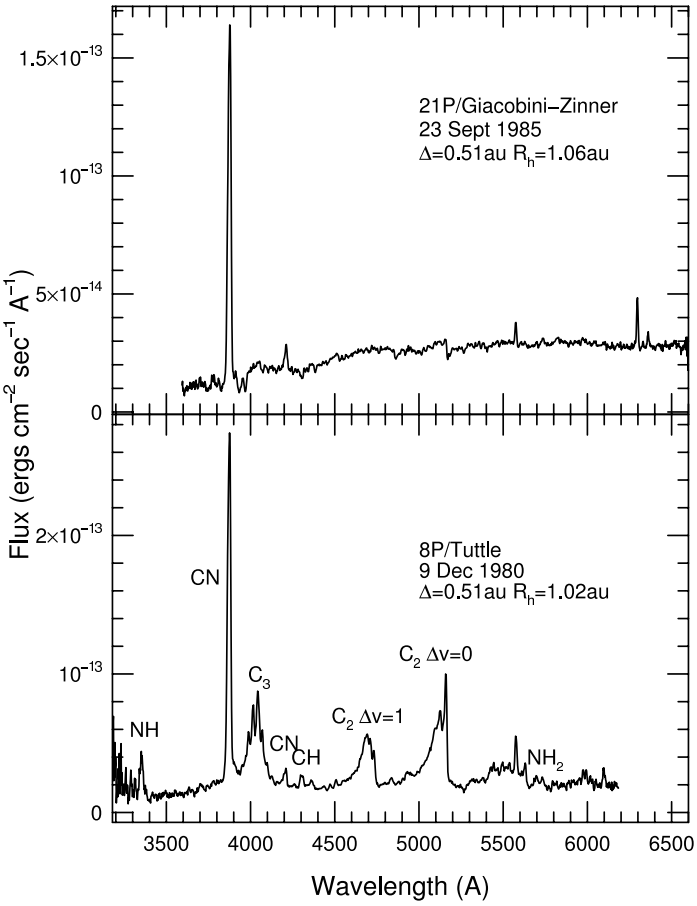

Figure 1: Spectra of 21P/Giacobini-Zinner and 8P/Tuttle obtained at McDonald Observatory are shown, scaled to the CN band at 3880Å. The comets were observed at comparable heliocentric and geocentric distances. Inspection of the figure shows that the well-defined C_2 and C_3 bands seen in Tuttle are nearly absent in Giacobini-Zinner's spectrum. (Spectra courtesy of A. Cochran)

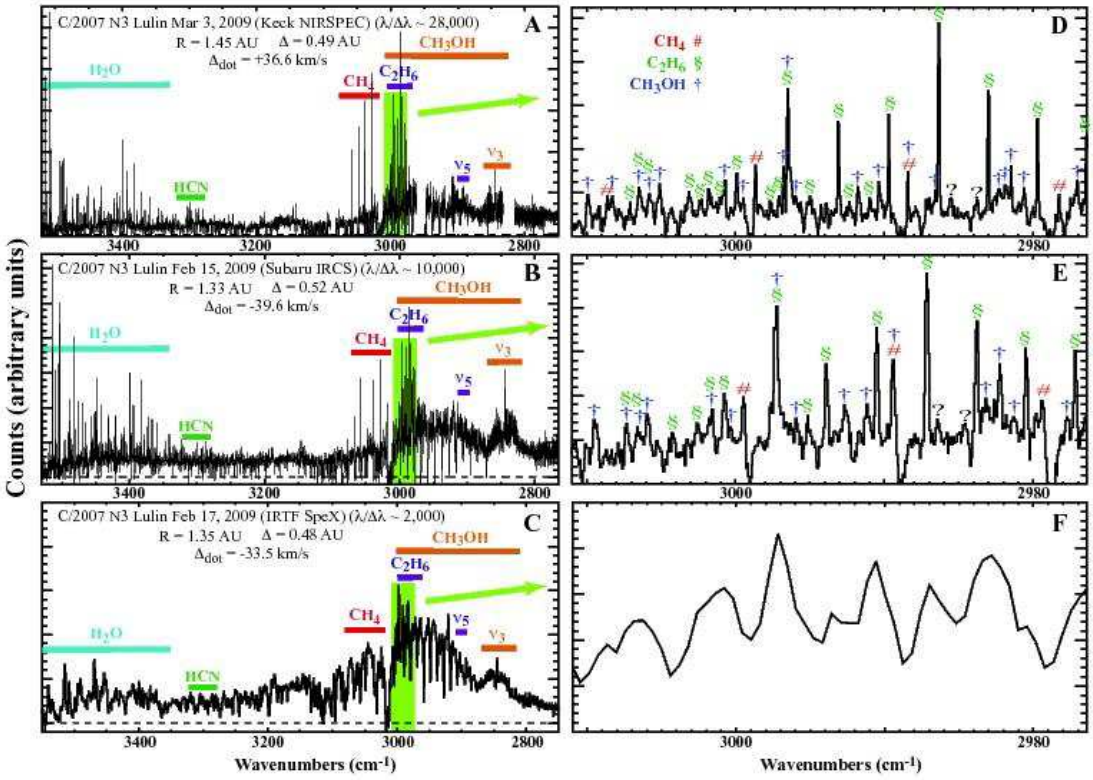

Figure 2: Direct comparison of high and moderate-resolution spectra for C/2007 N3 Lulin. Left panels show the complete spectra (before telluric correction) from $\sim 2.83 - 3.64$ μm ($\sim 3550 - 2750$ cm^{-1}). Right panels show a zoomed-in portion ($\sim 3.32 - 3.36$ μm) of these full spectra, as indicated by green boxes in the left figures. This illustrates two important points: (1) High-resolution spectra are necessary for the complete chemical interpretation of moderate-resolution spectra. (2) IR spectra are rich in cometary emissions underlining the importance of spectral surveys. Note that these spectra were obtained on different dates so the geocentric Doppler-shift is different (particularly for the NIRSPEC spectrum) so some lines are not present on all dates due to telluric extinction. (Spectrum courtesey N. Dello Russo)

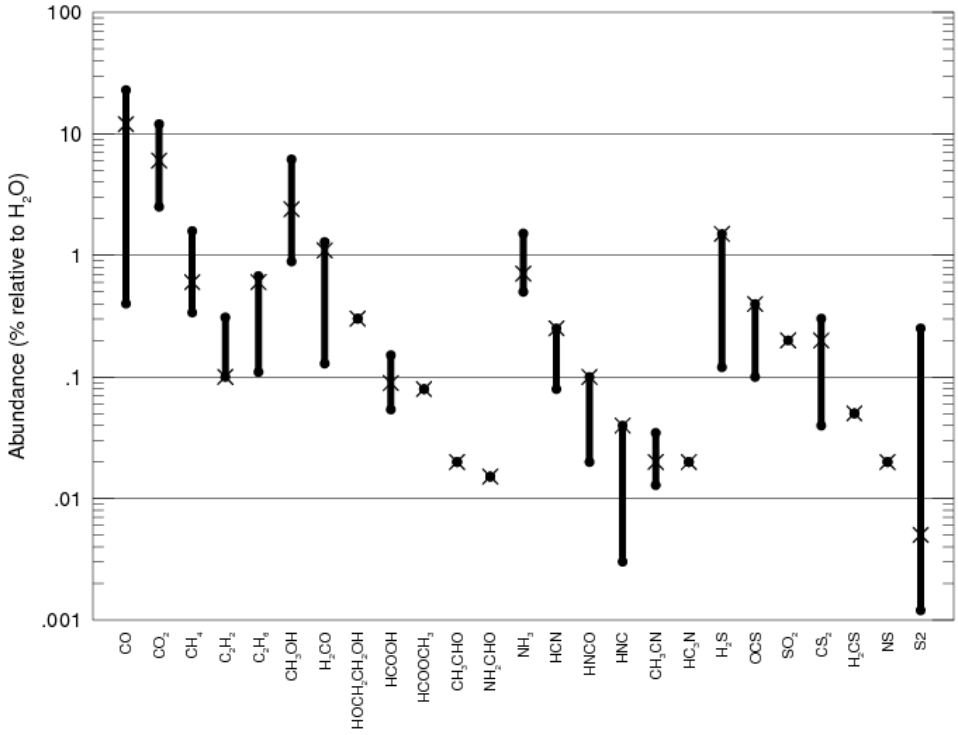

Figure 3: The abundances for many of the IR- and radio-observed species are shown as a percentage relative to water. The bar shows the range of values observed for each species. The "×" marks the value determined for comet C/1995 O1 (Hale-Bopp). CO, CH_3OH, H_2CO, HCN, H_2S and CS_2 were all observed in at least 10 comets; all other species where observed in fewer. The species with a single value (an X-dot) were only observed in Hale-Bopp (based on Figure 1 of Bockelée-Morvan 2011).

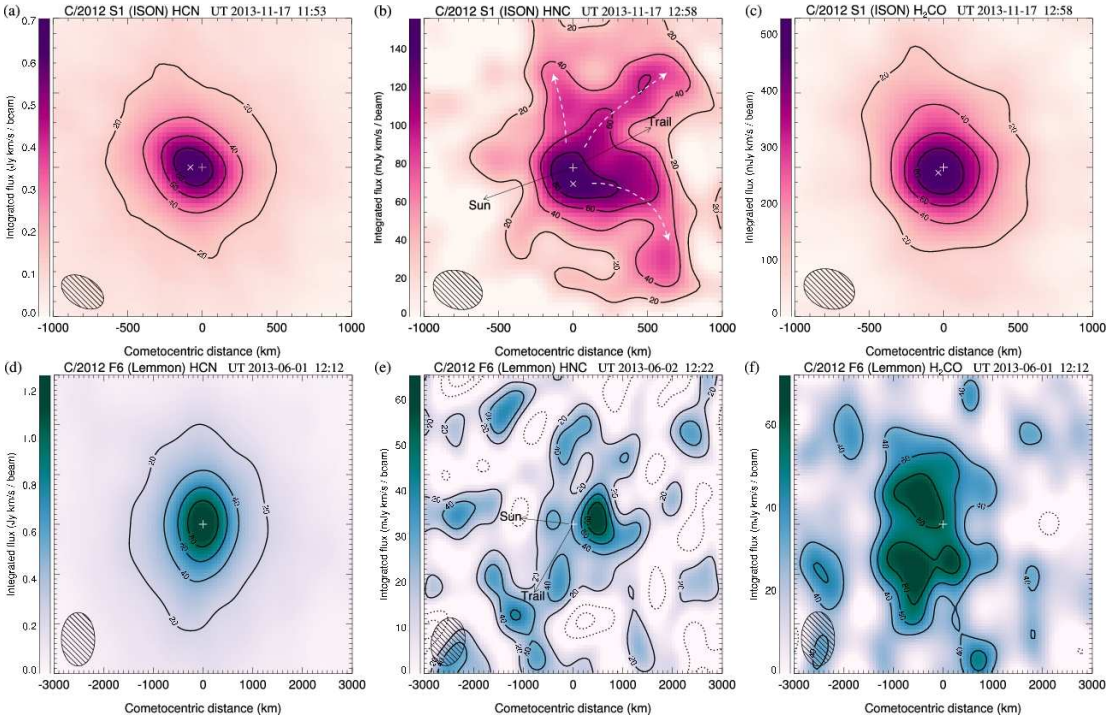

Figure 4: Contour maps of spectrally-integrated molecular line flux observed in comets S1/ISON (top row) and F6/Lemmon (bottom row). Contour intervals in each map are 20% of the peak flux. The 20% contour has been omitted from panel (f) for clarity. Negative contours are dashed. On panel (b), white dashed arrows indicate putative HNC streams/jets. The RMS noise (σ, in units of mJy beam^{-1} km s^{-1}) and contour spacings (δ) in each panel are as follows: (a) $\sigma = 10.9$, $\delta = 25.2\sigma$, (b) $\sigma = 13.6$, $\delta = 2.3\sigma$, (c) $\sigma = 11.0$, $\delta = 9.6\sigma$, (d) $\sigma = 13.1$, $\delta = 19.4\sigma$, (e) $\sigma = 14.8$, $\delta = 0.9\sigma$, (f) $\sigma = 13.7$, $\delta = 1.1\sigma$. The peak position of the (simultaneously observed) 0.9 mm continuum is indicated with a white '+'. For ISON, a white '×' indicates the integrated molecular emission peak position, offset from the continuum (dust) peak in each case. Sizes (FWHM) and orientations of the point-spread functions are indicated in lower-left (hatched ellipses); observation dates and times are also given. See Cordiner *et al.* (2014) for further details.

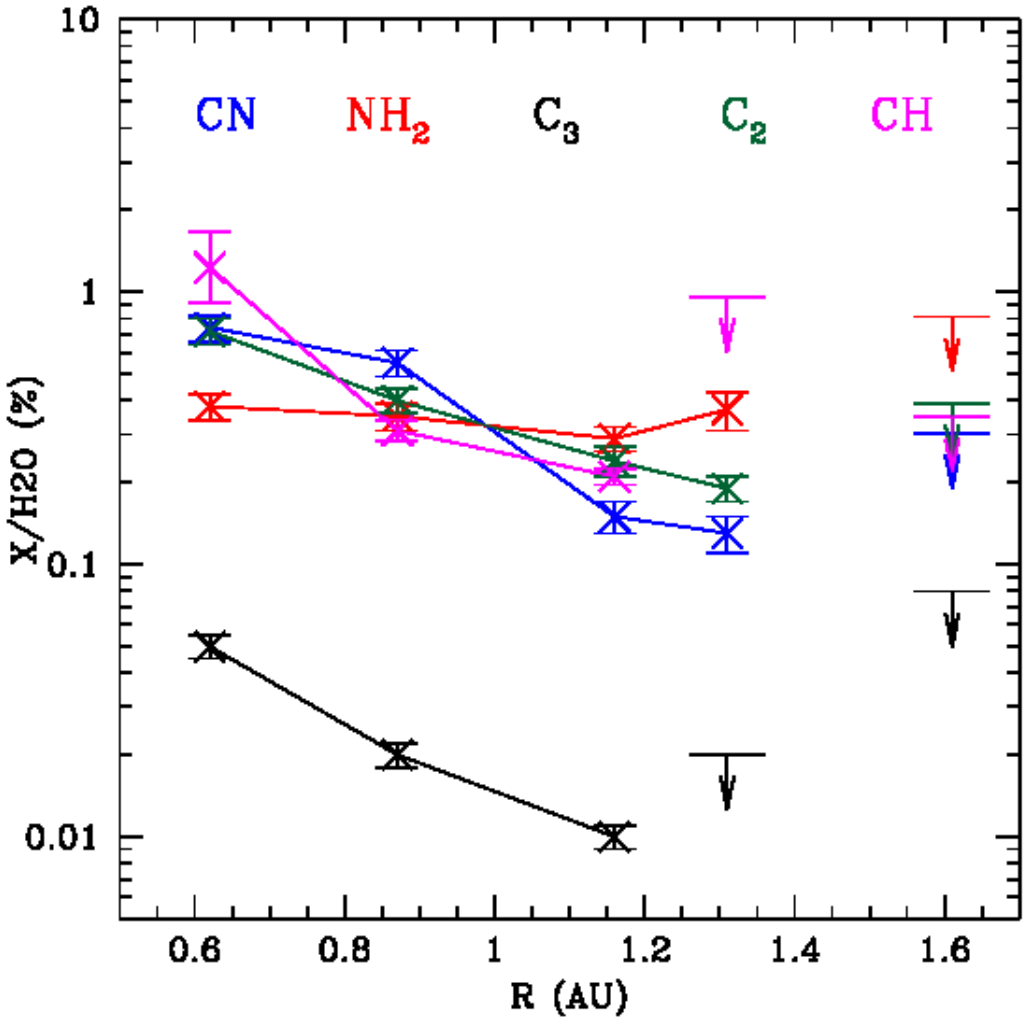

Figure 5: The mixing ratios of various fragment species are shown as a function of heliocentric distance for comet C/2012 S1 (ISON). The data were obtained with various telescopes but all are high spectral resolution observations. NH_2 shows no change relative to H_2O but the other species increased their fraction with respect to H_2O as the comet went from 1 AU to 0.6 AU.

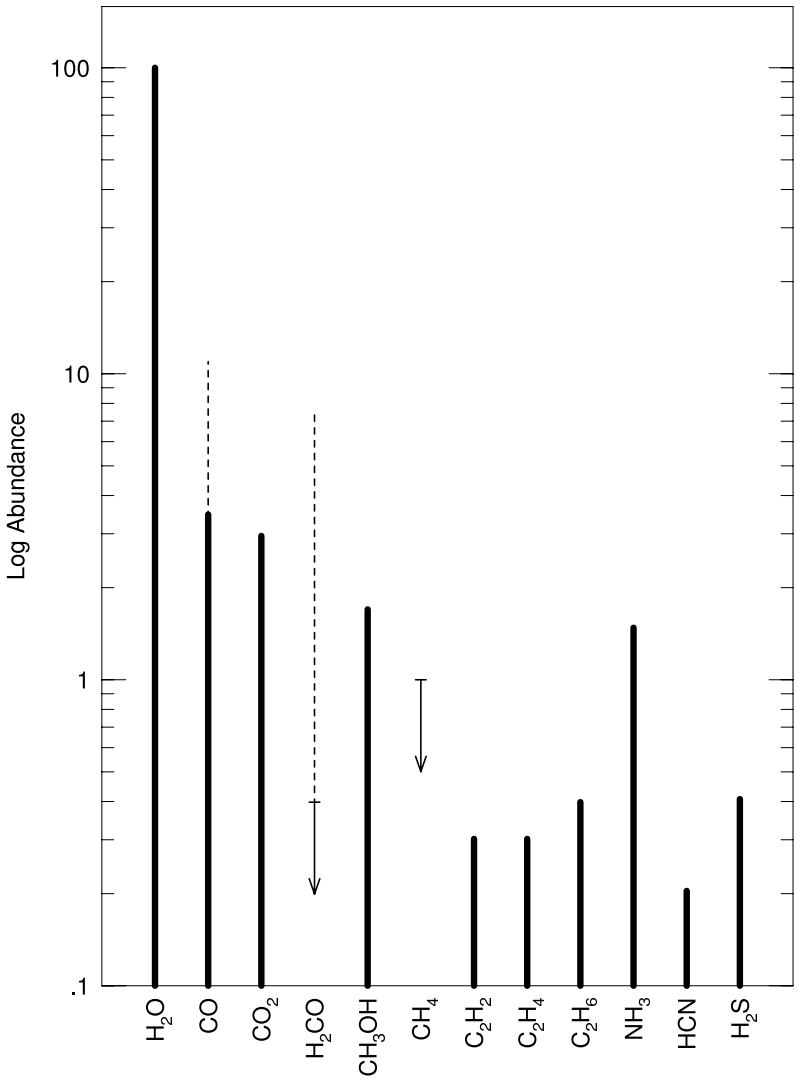

Figure 6: The abundances of various species that were detected with the mass spectrometers onboard the Giotto spacecraft are shown. Heavy solid lines show the abundances for species detected in comet 1P/Halley. Upper limits for the coma are shown with downward arrows. The lighter dashed lines show the additional contribution of the extended sources in the coma. However, note that Giotto's closest approach to the nucleus was 1100 km so some species could be produced by chemistry in the first 1100 km of outflow, while others may be released entirely or in part from the nucleus Based on Eberhardt (1999).

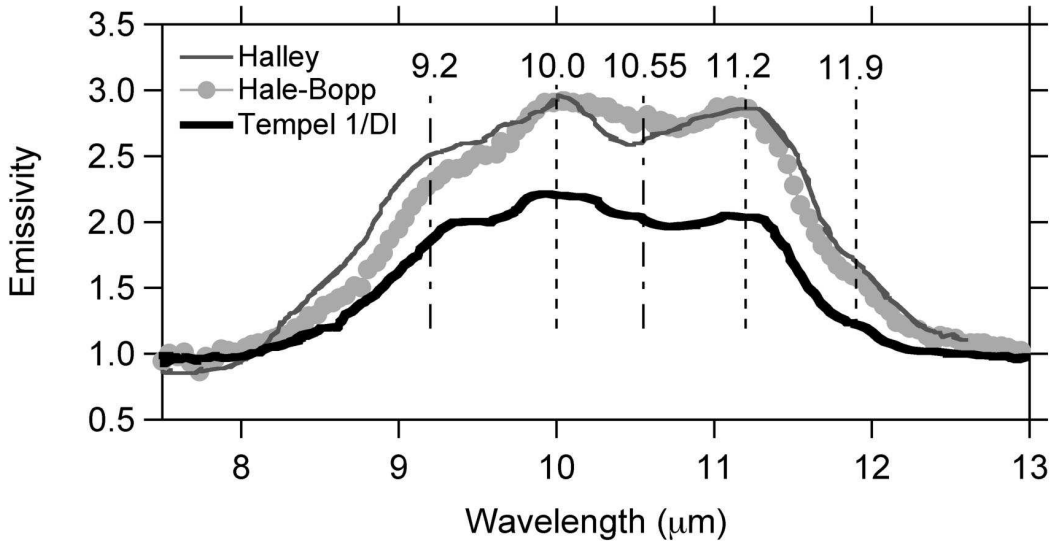

Figure 7: Comparison of silicate features, as observed for 1P/Halley and C/1995 O1 Hale-Bopp (adapted from Hanner, 1999), and for 9P/ Tempel 1 after the Deep Impact event and release of subsurface material (adapted from Kelley and Wooden, 2009). In each case the total flux is divided by the black body contribution. The main features are at 10 μm, 11.2 μm and 11.9 μm for crystalline olivine, and at 9.2 μm and 10.55 μm for crystalline ortho-pyroxene.

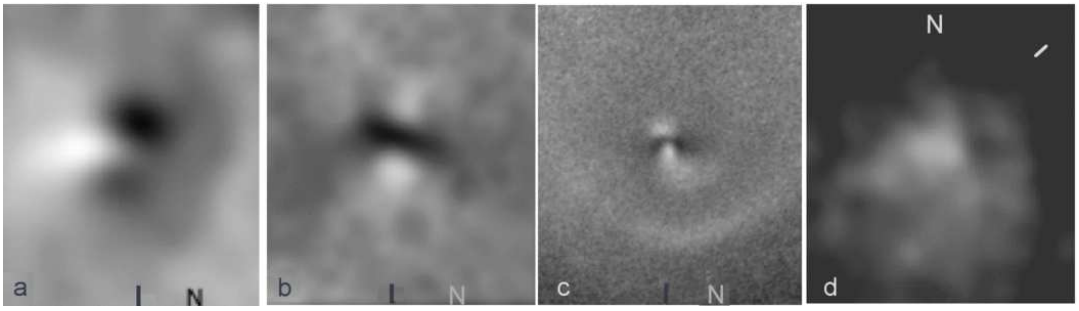

Figure 8: Evidence for different properties of solid particles in different regions of cometary comae, from linear polarization (P) maps at a given phase angle (α) a. Comet C/1990 K1 Levy at $\alpha = 18°$, in a field of view of 4000 km by 4000 km (black, P=-2.6%; white, P= 0.5%). b. Comet C/1995 O1 Hale-Bopp at $\alpha = 7°$, in a field of 38000 km by 38000 km (black, P=-6%; white, P=2%). c. Comet Hale-Bopp, now at $\alpha = 44°$, in a field of 82000 km by 82000 km (black, P= 9%; white, P= 18%). d. Comet 9P/Tempel 1, before Deep Impact event, without any conspicuous feature, at $\alpha = 41°$, in a field of 70000 km x 70000 km (black, P= 1%; white, P=10%). The solar direction is indicated by a black or white tick.

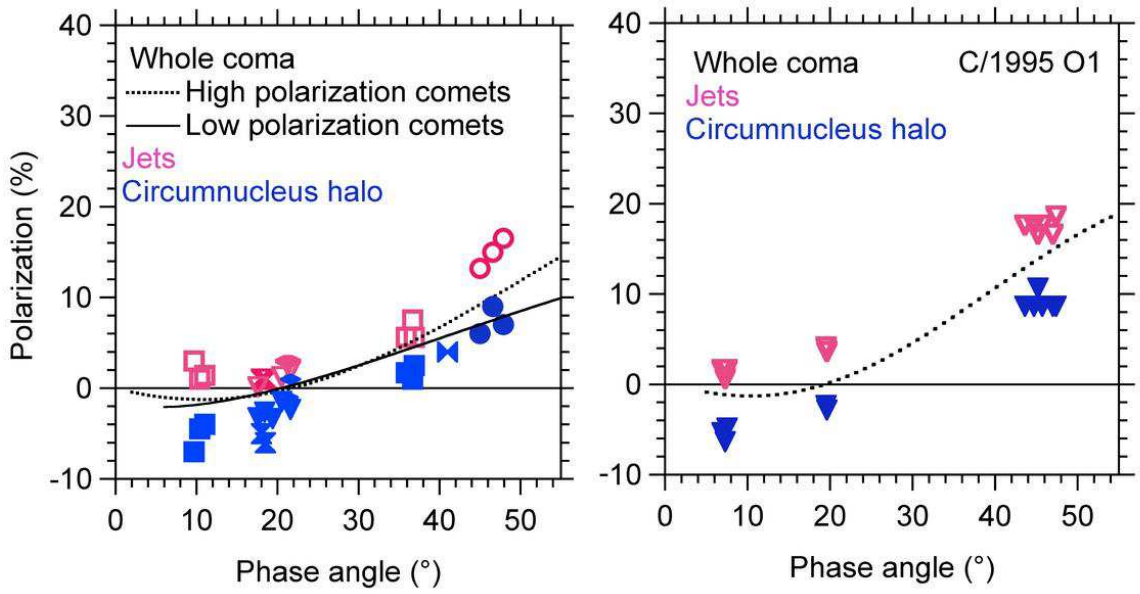

Figure 9: Evidence for changes in linear polarization, and thus in solid particle properties, within specific coma features (jets, circumnucleus polarimetric halo) observed at different phase angles. Left, comets with either high or low maxima in polarization; right, comet C/1995 O1 Hale-Bopp. While synthetic phase curves can be derived for whole cometary comae, the polarization is higher in jets (unfilled symbols) and lower in the circumnucleus halo (filled symbols), pointing out changes in composition and sizes (Updated from Hadamcik and Levasseur-Regourd, 2003b).